Chapter 6

Synthesis and mesomorphic properties of

(i) 2,7-Naphthylene bis(4-(E-4-*n*-alkoxy-α-methylcinnamoyl-oxy)-3-chlorobenzoates), (compounds 6.A.1 to 6.A.10)

(ii) 2,7-Naphthylene bis(4-(E-4-*n*-alkoxy-α-methylcinnamoyl-oxy)-3-methylbenzoates), (compounds 6.B.1 to 6.B.10)

6.1: Introduction

In continuation of the work on bent-core compounds exhibiting liquid crystalline phases, in this chapter, the synthesis and mesomorphic properties of BC compounds derived from 2,7-dihydroxynaphthalene are described. As mentioned earlier, compounds composed of bent-core (BC) molecules exhibit at least eight B mesophases [1-3] and some of these show ferroelectric or antiferroelectric switching behaviour [4, 5] despite the molecules being achiral. However, in some cases this type of BC molecules also exhibit calamitic phases such as nematic, smectic A and smectic C in addition to banana phase in the same compound [6-8]. In the case of bent-core compounds, the extensively studied central unit is a resorcinol moiety. The influence of a substituent in the central phenyl ring, and a systematic study of the effect of a lateral substituent on the middle phenyl as well as outer phenyl rings of bent-core compounds derived from resorcinol on the mesophase/s have been reported [9-11]. Thus, various phase sequence such as SmA-B_2, SmC-B_2, SmA-SmC-B_2, N-SmA-SmC-B_2 [6-8] have been observed in such systems.

The calamitic phase exhibited by bent-core compounds show unusual properties especially the nematic phase and it is considered to be important due to the possible phase biaxiality, interesting physical properties such as electrohydrodynamic instability, flexoelectric effect and their potential application in display devices. Interestingly, the formation of chiral domains of opposite handedness was observed in the nematic phase derived from 4-chlororesorcinol [12] and oxadiazole derivatives [13]. However, the combination of B-phases and calamitic phases are rare and these phases together can be obtained by bent-core compounds derived from 2,7-dihydroxynaphthalene central unit [14-18]. The influence of a lateral fluoro substituent on the mesophase behaviour of BC compounds derived from 2,7-dihydroxynaphthalene central unit was systematically investigated by Reddy *et al.* [14-15]. They found the interesting phase sequence of nematic to antiferroelectric B_2 phase and N to two-dimensional columnar phase (B_1), N to intercalated smectic phase (B_6) and N-Col_{ob} phase for the first time in systems containing esters of E-4-*n*-alkoxycinnamic acid and E-4-*n*-alkoxy-α-methylcinnamic acid in the side wings of BC compounds [14-15].

They also carried out a systematic study of the influence of a fluoro substituent in the middle phenyl ring as well as the terminal phenyl ring of BC compounds derived from 2,7-

dihydroxynaphthalene which showed various switchable phases [16-18]. All these compounds are symmetrical with respect to their central unit. The unsymmetrical bent-core compounds derived from 2,7-dihydroxynaphthalene system containing E-4-*n*-alkoxy-α-methylcinnamic acid group on one side also exhibited the nematic to Col_r and a nematic to B_2 phase [19] transition. The effect of different substituents on the mesophases of BC compounds containing 2,7-dihydroxynaphthalene central unit was also investigated by Svoboda *et al.* [20]. They found that the effect of Cl and CH_3 substituents on the mesophase was similar though the polarity is different whereas a CN substituent induced the novel B_7 phase. The nematic to polar columnar phase was reported by Kohout *et al.* [21] in the unsymmetrical BC compounds derived from 7-hydroxynaphthalene-2-carboxylic acid central unit.

The introduction of a fluorine lateral substituent is extensively studied in calamitic as well as BC systems compared to other lateral substituents such as chloro and methyl groups. Hence, we have chosen BC compounds composed of 2,7-dihydroxynaphthalene central unit containing of E-4-*n*-alkoxy-α-methylcinnamic acid group in the wings and chloro and methyl lateral groups on the middle phenyl ring for our studies. Thus, in this chapter the synthesis of two new homologous series of symmetric BC compounds containing chloro and methyl lateral substituents are described and their mesomorphic properties investigated. The general structure of compounds investigated is shown in structure **6**.

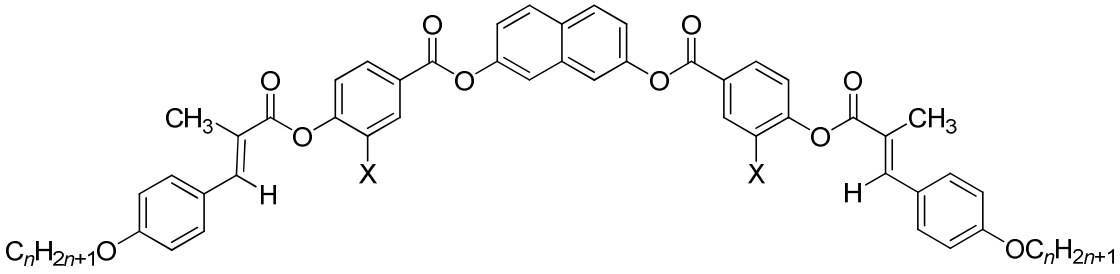

Structure 6

X = Cl	*n* = 8, 9, 10, 11, 12, 13, 14, 15, 16, 18	Series **6. A**
X = CH_3	*n* = 5, 6, 7, 8, 9, 10, 12, 13, 14, 16	Series **6. B**

6.2: Synthesis

The symmetric six-ring bent-core compounds derived from 2,7-dihydroxynaphthalene containing a chloro or a methyl lateral substitutent in the middle ring of the wings were synthesized following the synthetic pathway shown in scheme **6.2.** 3-Chloro/3-methyl-4-benzyloxybenzoic acid, **6.d** was prepared from 3-chloro/3-methyl-4-hydroxybenzoic acid, **6.a** following the procedure described in the literature and the synthetic route followed is shown in scheme **6.1**. 3-Chloro-4-hydroxybenzoic acid, **6.a** was obtained from Aldrich Pvt. Ltd. and the water of crystallization was removed before use. 3-Methyl-4-hydroxybenzoic acid was prepared following a procedure described in the literature [22] previously. 2,7-Dihydroxynaphthalene, **6.e**

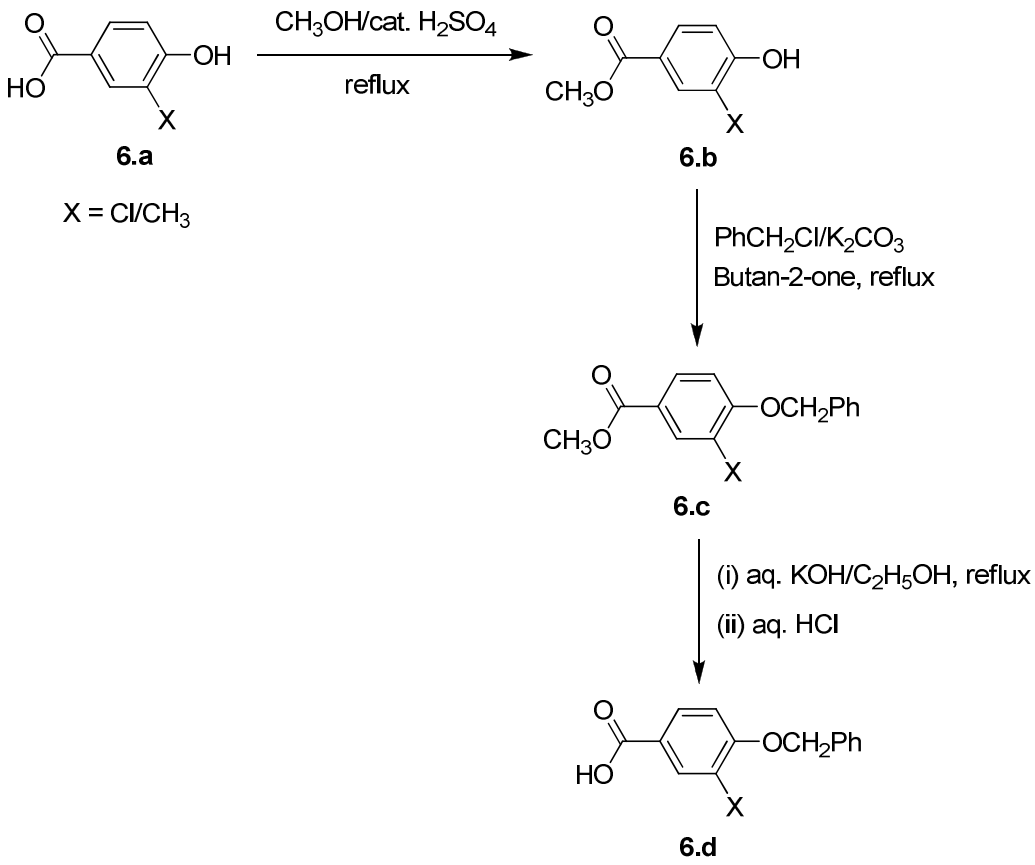

Scheme 6.1: Synthetic pathway employed for preparation of 3-chloro/3-methyl-4-benzyloxybenzoic acid 6.d.

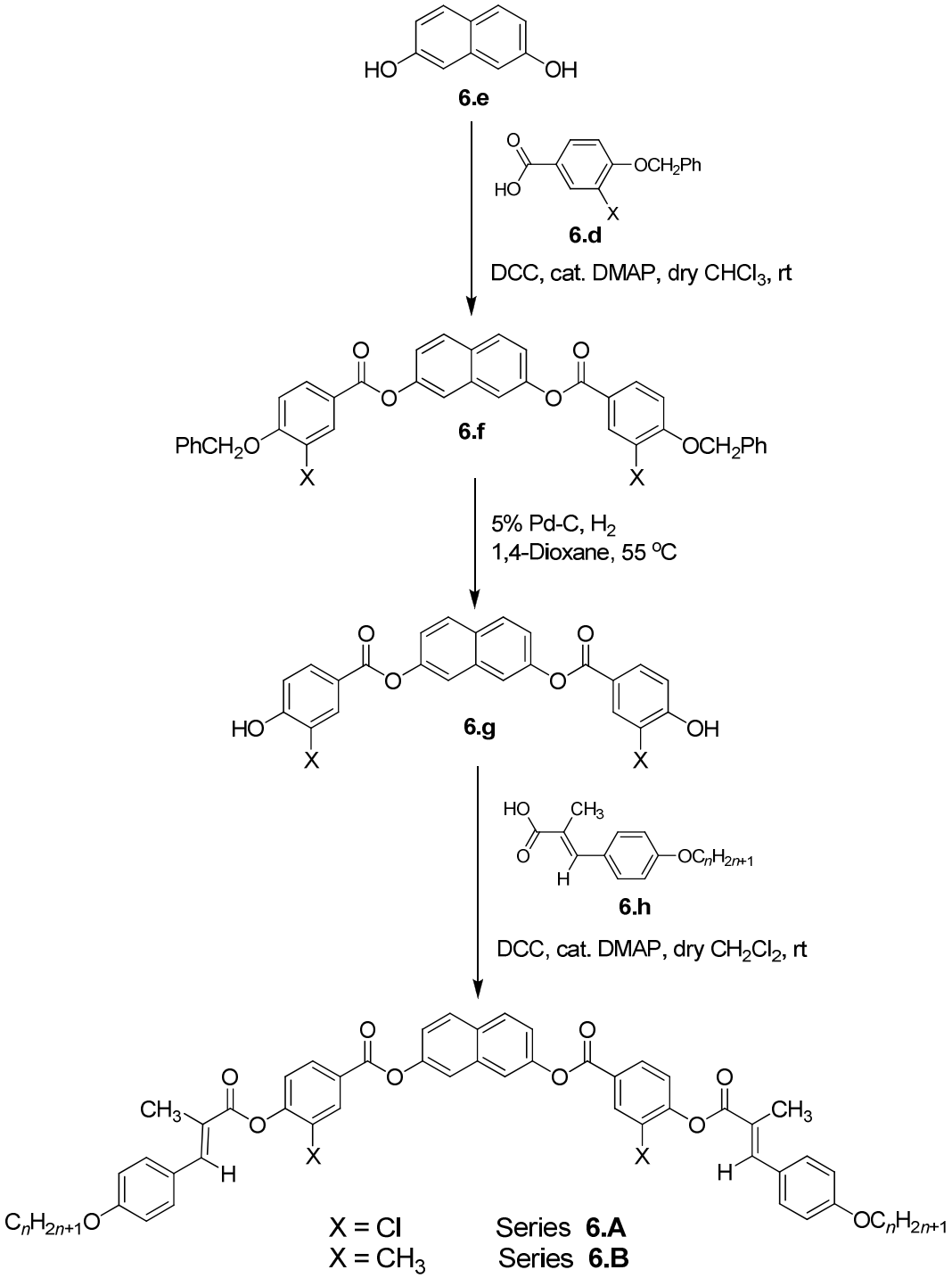

Scheme 6.2: Synthetic route followed for preparation of six-ring BC compounds of series 6.A and 6.B.

was also obtained commercially from Fluka and purified before use. 2,7-Dihydroxynaphthalene, **6.e** was treated with corresponding 3-chloro/3-methyl-4-benzyloxybenzoic acid, **6.d** in the presence of *N,N´*-dicyclohexylcarbodiimide (DCC) and a catalytic amount of 4-(*N,N*-dimethylamino)pyridine (DMAP) to obtain compound **6.f.** This protected diester compound **6.f** was subjected to hydrogenolysis in the presence of 5% Pd-C in 1,4-dioxane. The bisphenol, **6.g** thus obtained was purified and esterified with an appropriate E-4-*n*-alkoxy-α-methylcinnamic acid, **6.h** to obtain desired compounds of series **6.A** and **6.B.** E-4-*n*-alkoxy-α-methylcinnamic acids were prepared according to the procedure described in the literature [23].

6.3: Results and discussion

6.3.1: Mesomorphic properties

The transition temperatures and the associated enthalpy values obtained for two new homologous series of six-ring bent-core compounds **6.A** and **6.B** are summarized in tables **6.1** and **6.2** respectively. All the investigated compounds are mesomorphic in nature. As can be seen in table **6.1,** all compounds exhibit a nematic phase and all are enantiotropic. Compounds **6.A.1, 6.A.2, 6.A.3, 6.A.4** and **6.A.5** exhibit two mesophases, in which nematic phase is enantiotropic and a columnar phase is monotropic. A DSC thermogram obtained for compound **6.A.3** showing two transitions is depicted in figure **6.1.** It is noticed that the enthalpy values obtained for nematic to banana phase transition is relatively low and is of the order of 5-8 kJ mol^{-1}. When a sample of compound **6.A.3** was filled in the isotropic phase in a cell treated for planar alignment and cooled slowly, a nematic phase appears with two- and four-brush defects which then transformed into a texture as shown in figure **6.2.a.** On further cooling, a mosaic texture is formed and shown in figure **6.2.b** which is a typical texture for a two-dimensional rectangular columnar phase and similar optical textures were observed for other compounds **6.A.1, 6.A.2,** and **6.A.4** as well. Interestingly, compound **6.A.5** exhibited dendritic pattern on cooling into the lower temperature phase from nematic phase and the same is shown in figure **6.2.c.** Based on XRD measurements and electro-optical studies (described later) this

Table 6.1: Transition temperatures (T / °C) and enthalpies (ΔH/kJ mol^{-1}, in italics) for compounds of series 6.A[a]

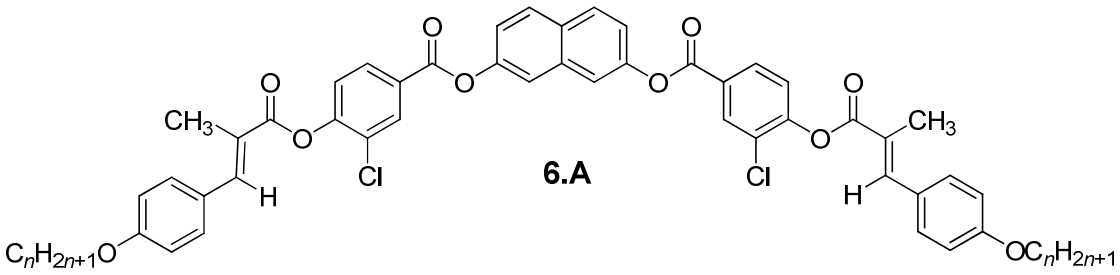

Compound	*n*	Cr		SmC′$_s$P$_A$		SmC$_s$P$_A$		SmCP$_A$		Col$_r$		N		I
6.A.1	8	•	113.5*	-		-		-		(•	89.0)	•	119.5	•
			72.1								*8.1*		*0.53*	
6.A.2	9	•	105.0*	-		-		-		(•	85.0)	•	113.5	•
			71.2								*7.2*		*0.44*	
6.A.3	10	•	96.5	-		-		-		(•	83.5)	•	111.0	•
			46.9								*7.0*		*0.45*	
6.A.4	11	•	96.0	-		-		-		(•	81.5)	•	108.5	•
			52.9								*6.6*		*0.37*	
6.A.5	12	•	98.5	-		-		-		(•	76.0)	•	106.0	•
			54.9								*5.5*		*0.41*	
6.A.6	13	•	93.5	-		-		(•	73.5)	-		•	104.0	•
			37.2						*4.6*				*0.39*	
6.A.7	14	•	94.0	-		-		(•	86.5)	-		•	104.5	•
			71.9						*5.7*				*0.40*	
6.A.8	15	•	97.0	-		-		(•	89.0)	-		•	104.5	•
			88.2						*5.3*				*0.38*	
6.A.9	16	•	96.5	(•	91.0)	(•	93.5)	-		-		•	104.0	•
			91.3		*0.29*		*4.1*						*0.43*	
6.A.10	18	•	95.5	(•	90.5)	•	100.0	-		-		•	103.5	•
			67.5		*0.25*		*4.0*						*0.48*	

[a]Abbreviations: Cr: crystalline phase; N: nematic phase; Col$_r$: columnar phase with rectangular lattice; SmCP$_A$: smectic C phase with antiferroelectric behaviour; SmC$_s$P$_A$: antiferroelectric smectic C phase with synclinic arrangement in the layers; SmC′$_s$P$_A$: variant of antiferroelectric smectic C phase with synclinic arrangement; I: isotropic phase; •: Phase exists; -: phase does not exist; *: compound has crystal-crystal transition and enthalpy denoted is the sum of all previous transitions; temperature in parenthesis indicates a monotropic transition.

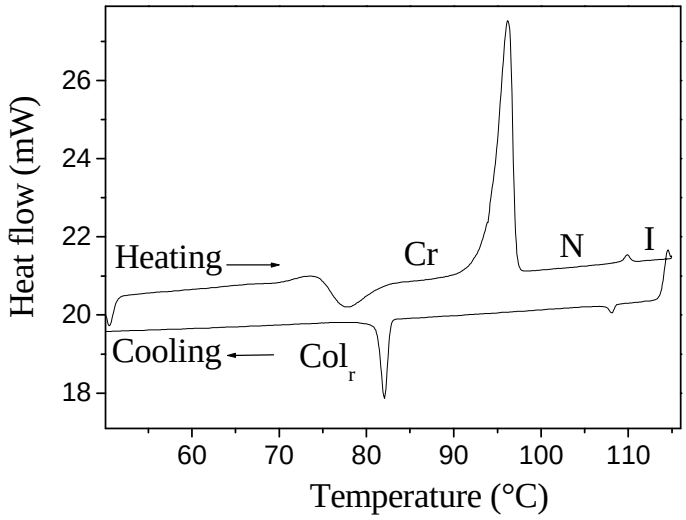

Figure 6.1: A DSC thermogram obtained for compound 6.A.3 showing transition to N and Col_r mesophases; scan rate 5 °C min^{-1}.

lower temperature mesophase has been characterized as a columnar mesophase with rectangular lattice (Col_r). Compound **6.A.3** exhibits the widest thermal range of 15 °C of nematic phase.

Interestingly, compounds **6.A.6, 6.A.7** and **6.A.8** are dimorphic in nature and exhibit polar smectic phase in addition to a nematic phase on increasing the chain length. When a thin film of a sample of compound **6.A.7** was sandwiched between two untreated glass plates and cooled slowly into mesophase from isotropic liquid, colourful schlieren texture was observed in the nematic phase under a polarizing microscope and this texture is shown in figure **6.3.a** and on further cooling, the lower temperature phase exhibits a schlieren texture mostly with four-brush defects which is shown in figure **6.3.b.** In the case of a homogeneously aligned cell, the nematic phase showed similar texture and this is shown in figure **6.2.a** for compound **6.A.3.** XRD measurements and electro-optical switching studies of middle homologues which are described later suggest that the lower temperature phase is a tilted smectic phase with antiferroelectric properties and the higher temperature phase is nematic. Hence the lower temperature mesophase of compounds **6.A.6, 6.A.7** and **6.A.8** are characterized as $SmCP_A$ phase. A DSC thermogram obtained for compound **6.A.7** is shown in figure **6.4** where the enantiotropic N to monotropic

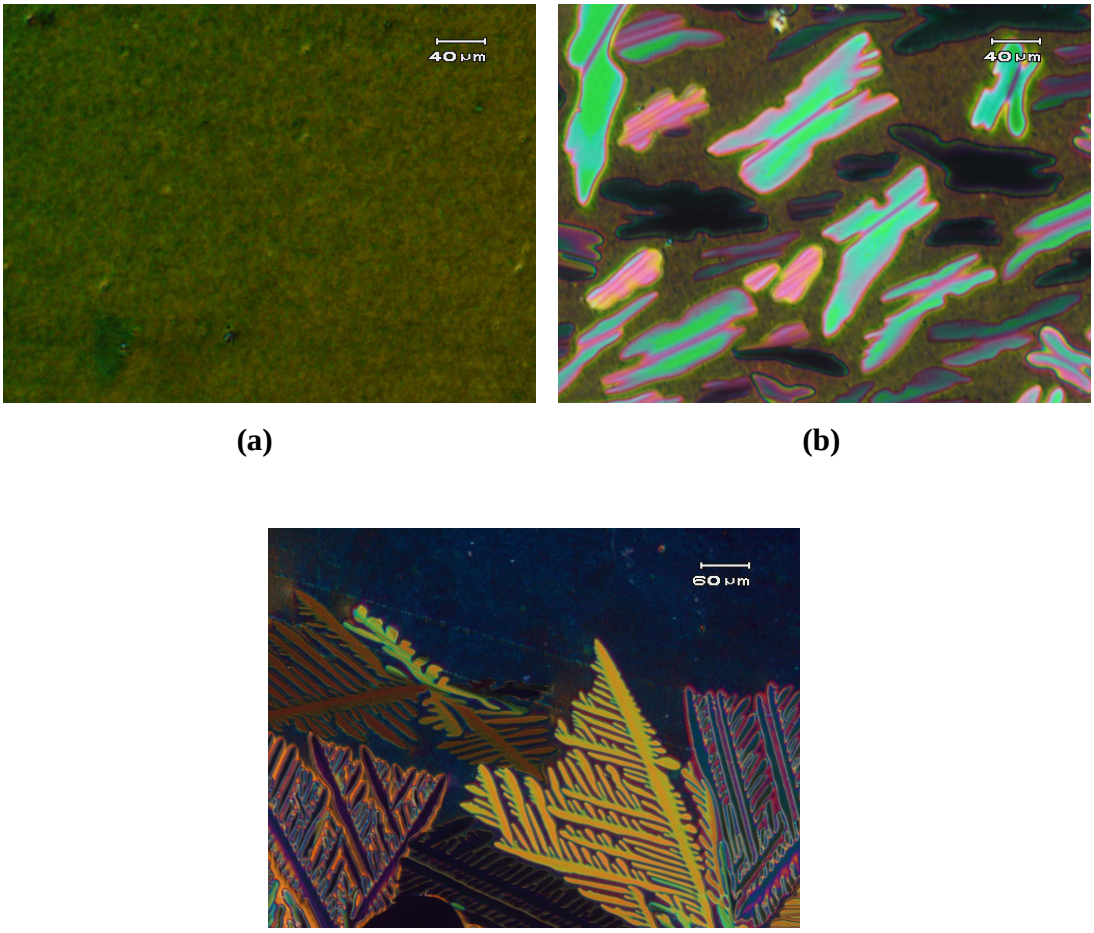

(a) **(b)**

(c)

Figure 6.2: Optical photomicrographs of nematic and Col_r mesophases in a cell treated for planar alignment. (a) Well aligned nematic texture at T = 105 °C; (b) mosaic texture of Col_r mesophase growing over nematic phase of compound 6.A.3 at T = 83.5 °C; (c) dendritic pattern of Col_r phase of compound 6.A.5 at T = 75.5 °C.

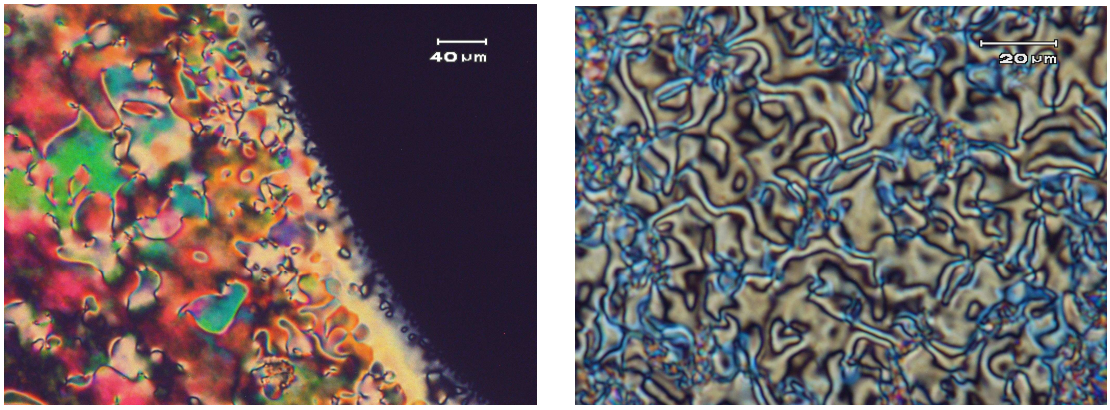

(a) **(b)**

Figure 6.3: (a) Optical texture of nematic phase appearing from isotropic phase of compound 6.A.7 at T = 103 °C; (b) the schlieren texture of $SmCP_A$ phase obtained on cooling the nematic phase, compound 6.A.7 at T = 83.7 °C.

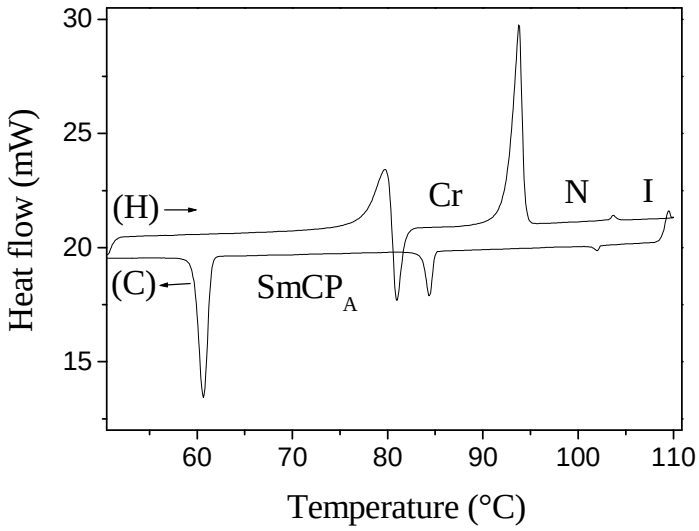

Figure 6.4: A DSC thermogram obtained for compound 6.A.7 showing transition to N and $SmCP_A$ mesophases; (H) heating cycle, (C) cooling cycle, scan rate 5 °C min^{-1}.

$SmCP_A$ phase transitions can be seen clearly. As mentioned earlier N to Col_r and N to $SmCP_A$ phase transitions have been observed in BC compounds derived from 2,7-dihydroxynaphthalene [14, 15].

Very interestingly, on increasing the terminal chain length compounds **6.A.9** and **6.A.10** are obtained which are trimesomorphic and show two polar smectic mesophases in addition to nematic phase. A DSC thermogram obtained for compound **6.A.10** showing nematic to two polar smectic phase transitions is depicted in figure **6.5.** The enthalpy value obtained for nematic to first antiferroelectric phase is similar to those of middle homologues. Though the enthalpy value is very low for the first antiferroelectric phase to second antiferroelectric phase transition, it can be seen clearly in the DSC thermogram. When a sample of compound **6.A.10** was filled in a cell treated for planar alignment in the isotropic phase and cooled slowly and viewed under a polarizing microscope, the nematic phase appeared first followed by a fan-shaped texture as shown in figure **6.6.a** and this suggests a synclinic arrangement in the smectic layers. On further cooling, a transition takes place with clear textural change which is shown in figure **6.6.b** and

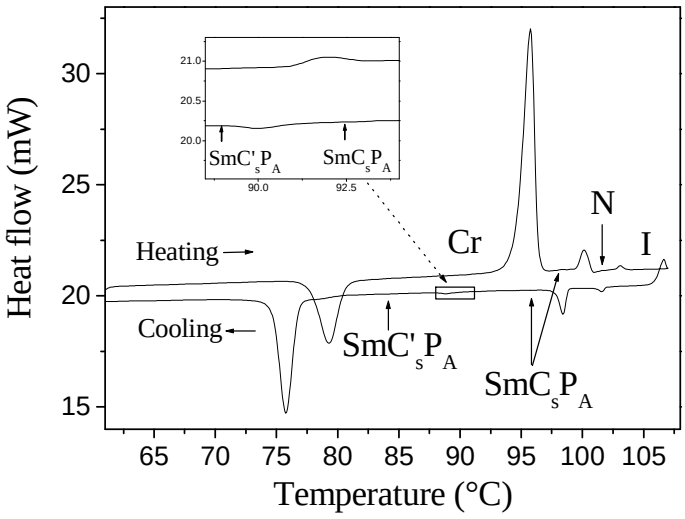

Figure 6.5: A DSC thermogram obtained for compound 6.A.10 shows transition from nematic to two antiferroelectric phases; scan rate 5 °C min^{-1}.

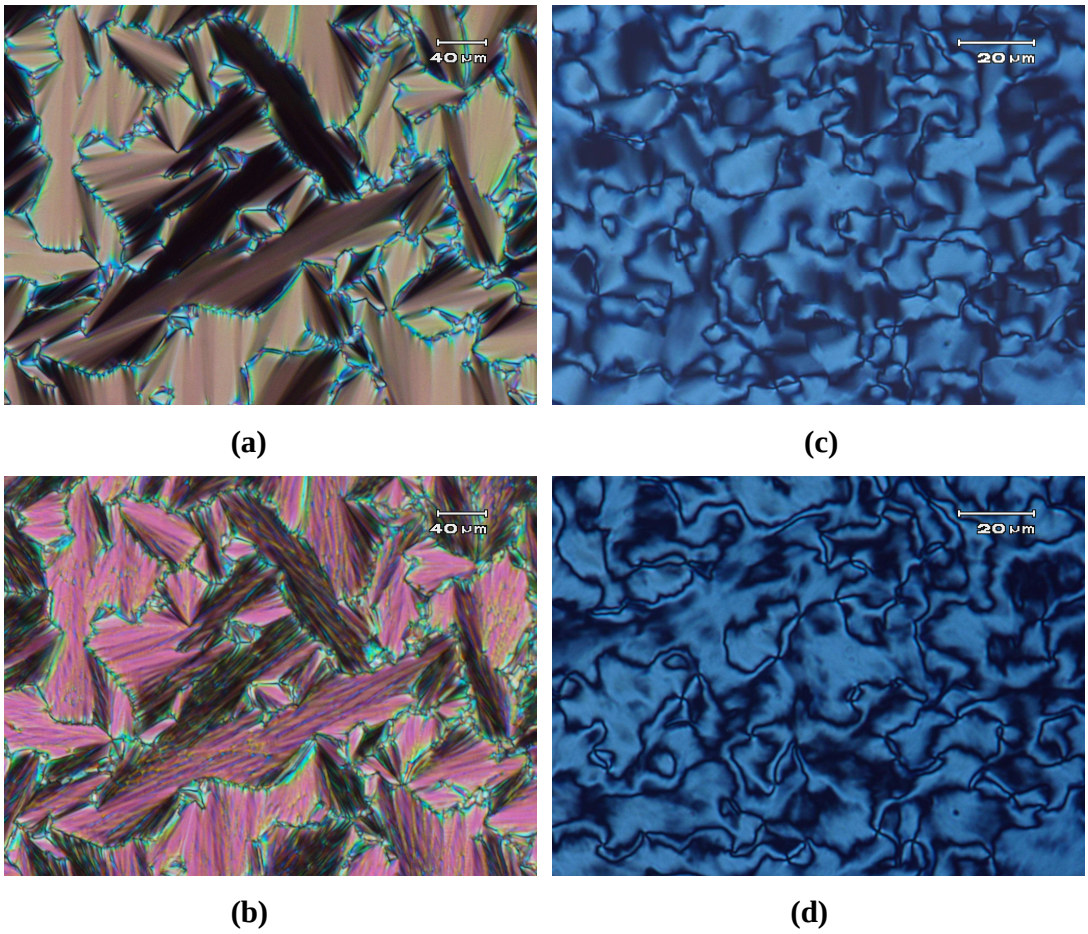

Figure 6.6: Photomicrograph of optical textures of compound 6.A.10 obtained in the planar cell cooling from nematic phase (a) SmC_sP_A phase at T = 97 °C; (b) SmC'_sP_A phase at T = 87 °C; Schlieren textures of (c) SmC_sP_A phase at T = 95 °C; and (d) SmC'_sP_A phase at T = 85 °C of same compound observed in a cell treated for homeotropic alignment.

this is also synclinic. When the same sample was viewed in a cell treated for homeotropic alignment and cooled slowly, the nematic phase transformed to a schlieren texture and the photomicrographs of optical textures obtained in the lower and lowest temperature mesophases are shown in figures **6.6.c** and **6.6.d** respectively.

Electro-optical switching studies confirmed that the lower temperature smectic mesophases are antiferroelectric in nature. XRD measurements on lower temperature phases were not possible as the sample crystallized rapidly. On the basis of optical textures and electro-optical switching studies as described later, the lower temperature mesophases have been characterized as SmC_sP_A and SmC'_sP_A phases. Similar optical textures were obtained and switching behaviour observed for compound **6.A.9** as well.

A plot of transition temperatures against the number of carbon atoms in the alkoxy chain for this homologous series is shown in figure **6.7.** It can be seen that there is a gradual decrease in the nematic to isotropic transition which levels off as the series is ascended. Whereas falling curve is observed for N to Col_r phase transition and a rising curve is seen for N to $SmCP_A$ phase transitions on ascending the series.

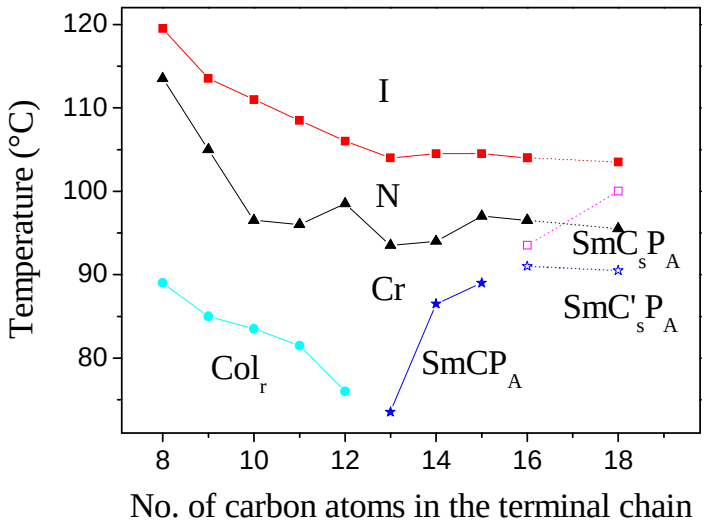

Figure 6.7: A plot of transition temperature as a function of number of carbon atoms in the terminal chain for compounds of series 6.A.

Table 6.2: Transition temperatures (T / °C) and enthalpies (ΔH/kJ mol^{-1}, in italics) for compounds of series 6.B[a]

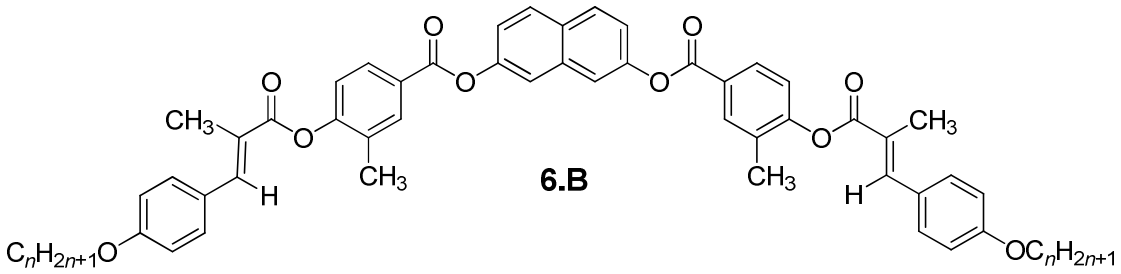

Compound	*n*	Cr		SmC		N		I
6.B.1	5	•	138.5*	(•	75.5)	(•	137.5)	•
			62.7		*0.25*		*0.86*	
6.B.2	6	•	120.0*	(•	76.0)	•	133.5	•
			93.4		*0.27*		*0.98*	
6.B.3	7	•	112.5*	-		•	123.5	•
			144.8				*0.77*	
6.B.4	8	•	113.5*	-		•	119.5	•
			112.3				*0.91*	
6.B.5	9	•	112.5*	-		(•	112.0)	•
			66.1				*0.69*	
6.B.6	10	•	111.0*	-		(•	108.5)	•
			56.5				*0.66*	
6.B.7	12	•	114.0*	-		(•	103.0)	•
			65.9				*0.55*	
6.B.8	13	•	111.5	-		(•	98.0)♠	•
			65.6					
6.B.9	14	•	111.5*	-		(•	96.0)♠	•
			44.8					
6.B.10	16	•	116.5*	-		(•	92.5)♠	•
			65.9					

[a] See **Table 6.1**: SmC: calamitic smectic C phase; ♠: mesophase observed only under microscope and not seen in DSC; enthalpy value could not be determined as the sample crystallizes immediately.

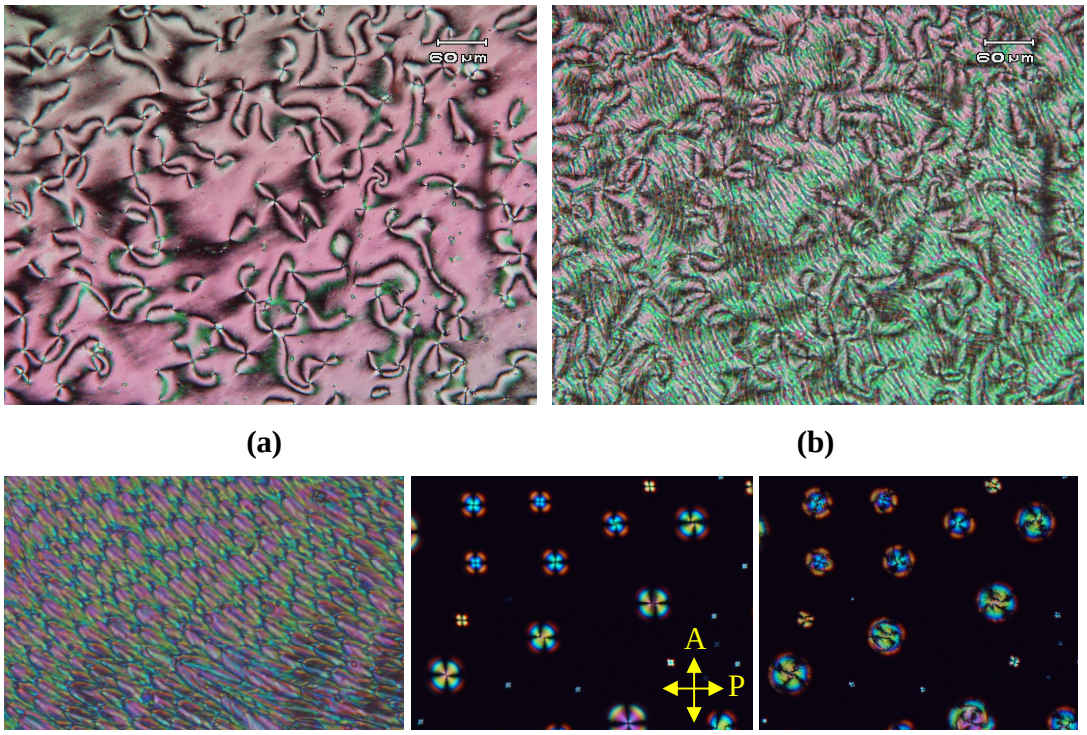

(a) **(b)**

(c) **(d)** **(e)**

Figure 6.8: (a) Optical textures obtained for compound 6.B.2 on cooling from the isotropic phase (a) Nematic phase at T = 110 °C; (b) SmC phase at T = 70 °C on cooling from nematic phase in a homeotropically aligned cell; (c) completely formed SmC phase in different region at T = 65 °C; droplets formed on the glass plates showing dark brushes in (d) & (e) nematic and SmC phases respectively and the brushes rotate in (e).

For comparison purposes we have synthesized another series of compounds **6.B** containing a lateral methyl substituent in the middle ring of the arm. The transition temperatures together with enthalpy values for this series of compounds are summarized in table **6.2.** As can be seen from table **6.2,** all compounds exhibit a nematic phase. Compounds **6.B.1** and **6.B.2** are dimesomorphic and show SmC phase in addition to a nematic phase. When a thin film of a sample of compound **6.B.2** filled in a cell treated for homeotropic alignment in the isotropic

phase and cooled slowly, the nematic phase exhibited the birefringent schlieren texture which is shown in figure **6.8.a.** On further cooling a transition takes place and a typical texture obtained during the transition is shown in figure **6.8.b.** The texture of the lower temperature phase obtained in different regions of the cell is also shown figure **6.8.c** which is indicative of a smectic phase. In order to understand the nature of this smectic phase, droplets formed on the glass plate in the nematic phase were observed carefully during transition and a typical photomicrograph obtained is shown in figure **6.8.d.** The extinction brush of droplets are inclined to polarizer and analyzer which is crossed and cooling into lower temperature phase, the dark brushes rotate to some extent indicating a synclinic arrangement of molecules in the neighbouring layers and the optical texture obtained is shown in figure **6.8.e.** The lower temperature mesophase of compound **6.B.2** could not be aligned homeotropically thus the possibility of this phase being SmA is ruled out and also this phase does not respond to an applied electric field. These textural observations and electro-optical switching studies suggest that the lower temperature phase is a smectic C phase with synclinic arrangement of the molecules. Compound **6.B.2** exhibited

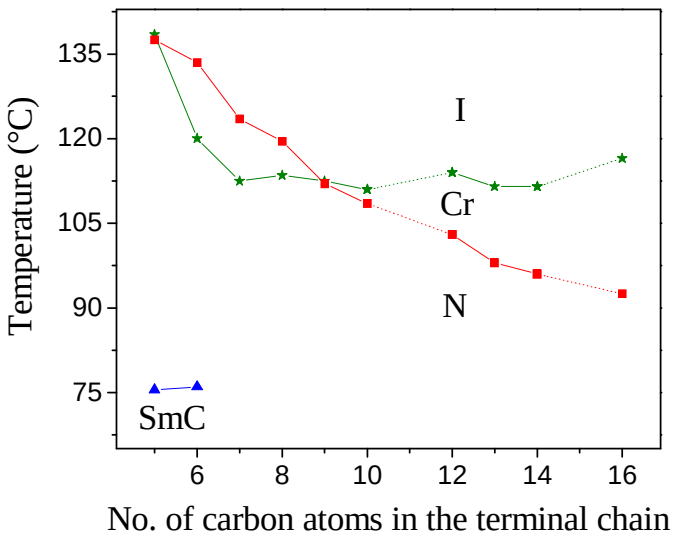

Figure 6.9: A plot of transition temperature *vs* number of carbon atoms in the terminal chain for compounds of series 6.B.

enantiotropic nematic phase and monotropic SmC phase. Similarly compound **6.B.1** showed the same phase sequence where both the mesophases are monotropic.

Other homologues **6.B.3** to **6.B.10** are monomesomorphic and show only nematic phase. Compounds **6.B.4** and **6.B.5** are enantiotropic and on increasing the chain length further, the mesophase is destabilized and as a result it becomes a highly metastable nematic phase. Among all these compounds of series **6.B,** compound **6.B.2** showed the widest thermal range of 12.5 °C of the nematic phase. However, the nematic phase could not be aligned homeotropically in both the series of compounds. A plot of transition temperature as a function of carbon atoms in the terminal chain for this series is shown in figure **6.9**. A falling curve is seen for nematic to isotropic transition on ascending the series.

6.3.2: X-Ray diffraction measurements

In order to determine the structure of the mesophases, we have carried out powder XRD measurements on the mesophases of compounds of series **6.A** and **6.B.** For example, a sample of compound **6.A.4** was filled in a Lindemann capillary (dia: 0.7 mm) in the isotropic state and the ends were sealed carefully. This sample was cooled slowly into the lower temperature mesophase and on irradiation, a typical intensity profile was obtained, and this is shown in figure **6.10.a.** A diffuse wide angle peak at about 4.7 Å indicating a liquid-like order was also obtained. The d-spacings in the small angle region correspond to d_1 = 32.52 Å, d_2 = 27.07 Å, d_3 = 16.64 Å, and d_4 = 13.64 Å. These reflections could be indexed as 11, 02, 22, and 04 planes of a two-dimensional columnar rectangular lattice and the lattice parameters obtained are a = 40.69 Å and b = 54.14 Å. One of the lattice parameters b is related to the measured molecular length (L = 57.3 Å). Similar diffraction patterns were obtained for compounds **6.A.1** and **6.A.3** and the XRD data obtained are listed in table **6.3.**

The X-ray diffractrogram obtained in the lower temperature $SmCP_A$ phase of compound **6.A.7** is given in figure **6.10.b**. Three sharp reflections were seen in the small angle region at d_1 = 42 Å, d_2 = 21 Å and d_3 = 14 Å. These reflections are in the ratio of 1 : ½ : ⅓ suggesting a lamellar ordering in the mesophase. The first order layer spacing was found to be smaller than

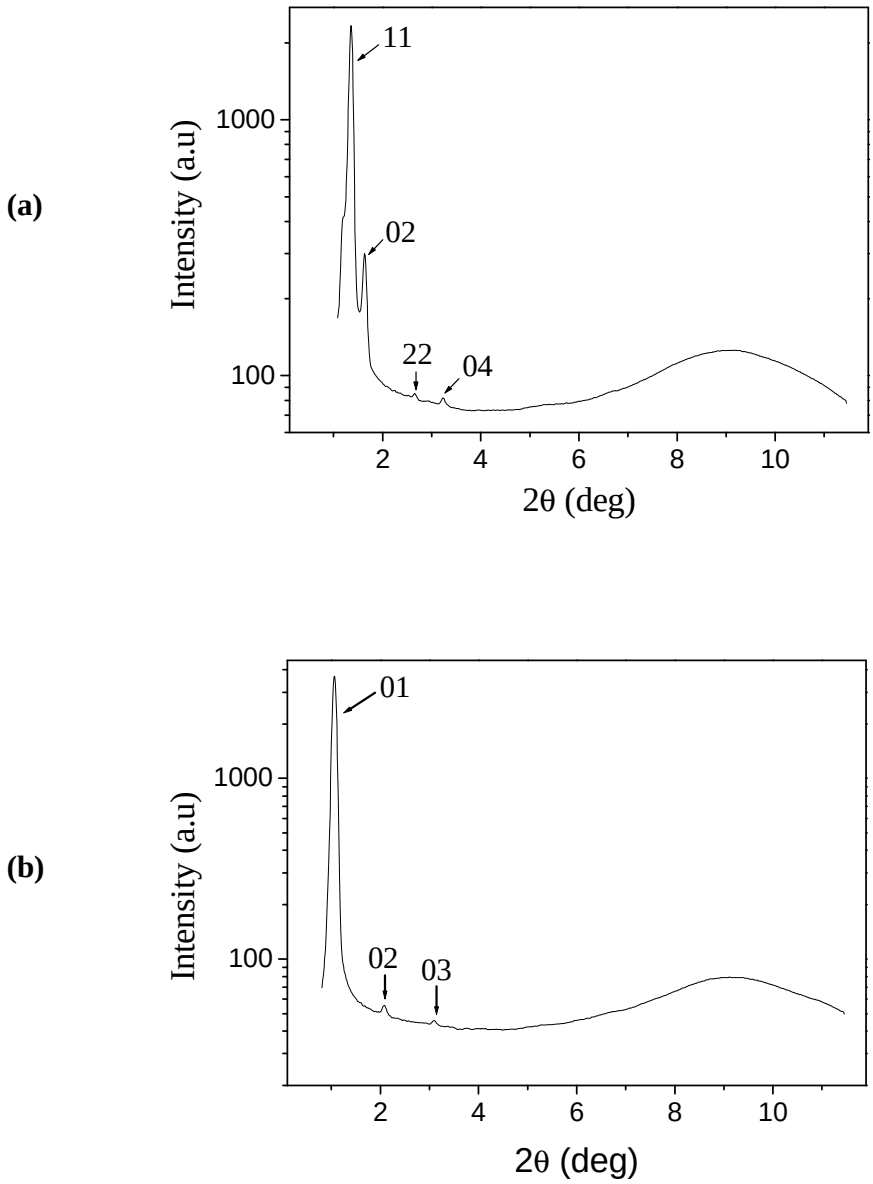

Figure 6.10: XRD intensity profile obtained for compounds 6.A.4 and 6.A.7 in the (a) Col_r phase at T = 78 °C and (b) $SmCP_A$ phase at T = 80 °C respectively.

Table 6.3: The d-spacings (Å) obtained for the mesophases of different compounds belonging to series 6.A; the corresponding Miller indices are shown in brackets.

Compound	d-spacings/Å(Miller indices)	Lattice parameters/Å		Meso-phase	T/°C
		a	b		
6.A.1	28.5 (11), 25.17 (02), 12.58 (04)	34.57	50.34	Col_r	85
6.A.3	30.04 (11), 25.51 (02), 12.94 (04)	37.16	51.02	Col_r	80
6.A.4	32.52 (11), 27.07 (02), 16.64 (22), 13.64 (04)	40.69	54.14	Col_r	78
6.A.7	42 (01), 21 (02),14 (03)	-	-	$SmCP_A$	80
6.A.8	43.68 (01), 22 (02), 14.8 (03)	-	-	$SmCP_A$	83
6.A.9	45 (01)	-	-	SmC_sP_A	85
6.A.10	46 (01)	-	-	SmC_sP_A	95

the measured molecular length assuming an all-*trans* conformation of the terminal *n*-alkoxy chain (L = 63 Å for compound **6.A.7**) suggesting a tilt of the molecules in the mesophase with a tilt angle of 48°. Compound **6.A.8** also showed a similar diffraction pattern. Unfortunately, we could not carry out X-ray measurements in detail for compounds **6.A.9** and **6.A.10** as the samples crystallized rapidly. However, we could get only one reflection in the small angle region for the first antiferroelectric phase of compounds **6.A.9** and **6.A.10**. The d-spacings obtained in the mesophases are given in table **6.3**. The diffuse scattering in the wide angle region pointing liquid-like ordering is seen in all the cases. However, XRD measurements of the lower temperature SmC phase of compounds **6.B.1** and **6.B.2** were also not possible as it is a

highly metastable phase. The nematic phase could easily be identified by optical textures for both the series of compounds.

6.3.4: Electro-optical studies

The electro-optical behaviour of the mesophases exhibited by compounds of series **6.A** were examined in EHC cells (cell thickness, 8 µm) by using the triangular-wave method. These EHC cells are constructed using conducting glass plates which are precoated with polyimide and unidirectionally rubbed for planar alignment. When a representative sample of compound **6.A.7** was taken in a cell and cooled slowly down to smectic phase, a grainy texture appeared. On applying a triangular voltage, above the threshold a fan-shaped texture was obtained and this is shown in figure **6.11.b.** Simultaneously, two polarization current peaks per half cycle of the applied voltage could be seen in the oscilloscope and a typical current response obtained by applying appropriate triangular-wave voltage of 386 V_{pp} and frequency of 20 Hz at T = 79 °C is shown in figure **6.11.a.** The optical textures obtained under the field and in absence of the field are shown in figures **6.11.b** and **6.11.c** respectively. The saturated polarization value for $SmCP_A$ phase of compound **6.A.7** was determined to be about 700 nC cm^{-2}. However, the dark extinction cross was found to be parallel to the direction of crossed polarizer and analyzer indicating an anticlinic arrangement of molecules under the ac field. The dc field experiment did not give any information about arrangement of the layers as it always formed grainy textures.

Similarly, the switching behaviour of compound **6.A.10** was carried out in EHC cell having a thickness of 8 µm. A sample was cooled to lower temperature phase from nematic phase when bright fan-shaped texture appeared. On applying a triangular-wave voltage, change in birefringence was observed and as a result the field of view became green in colour. Two peaks per half cycle of the applied voltage were observed in current response trace indicating an antiferroelectric behaviour and at a voltage of 256 V_{pp} and a frequency of 4 Hz, the peaks saturated. The current response trace obtained in the lower temperature phase is shown in figure **6.12.a** and the optical textures obtained with field and without field are shown in figures **6.12.b** and **6.12.c** respectively. On further cooling to the lowest temperature phase under the same conditions, two current peaks per half cycle were observed with a change in peak position and

(a)

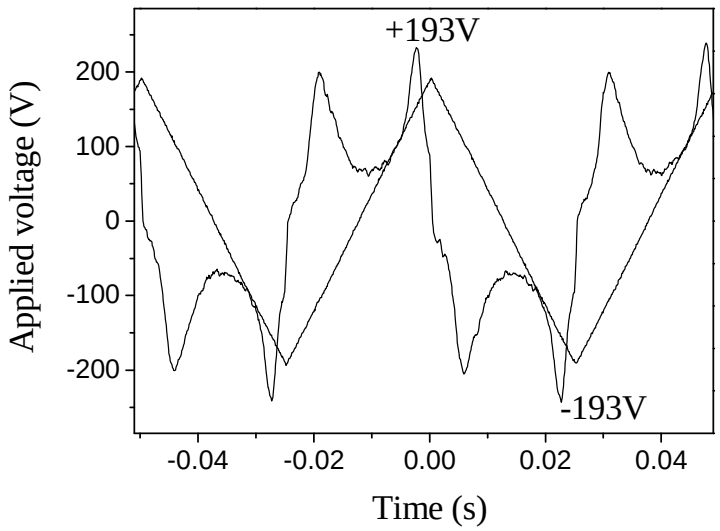

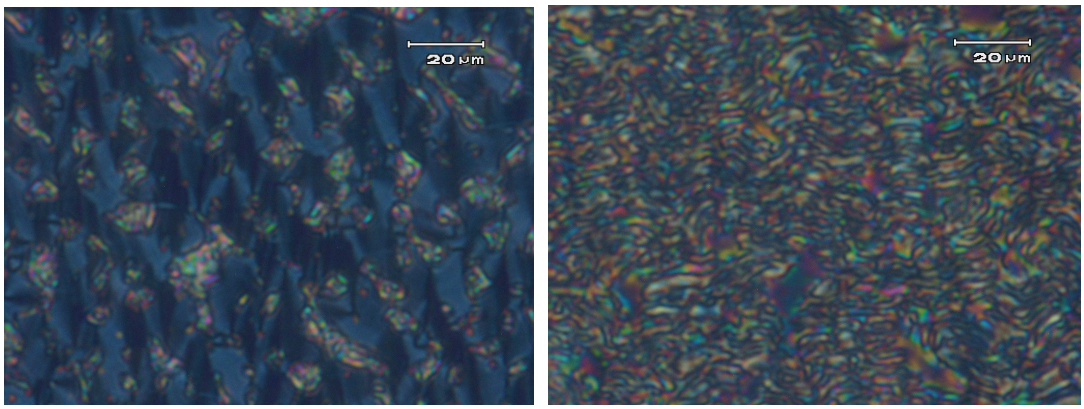

(b) **(c)**

Figure 6.11: (a) Switching current response trace obtained in the lower temperature $SmCP_A$ phase of compound 6.A.7 on applying a triangular-wave electric field, at T = 79 °C; 20 Hz; 386 V_{pp}; $P_S \approx 700$ nC cm^{-2}. Photomicrographs obtained in the $SmCP_A$ phase (b) under the electric field and (c) without the electric field.

(a)

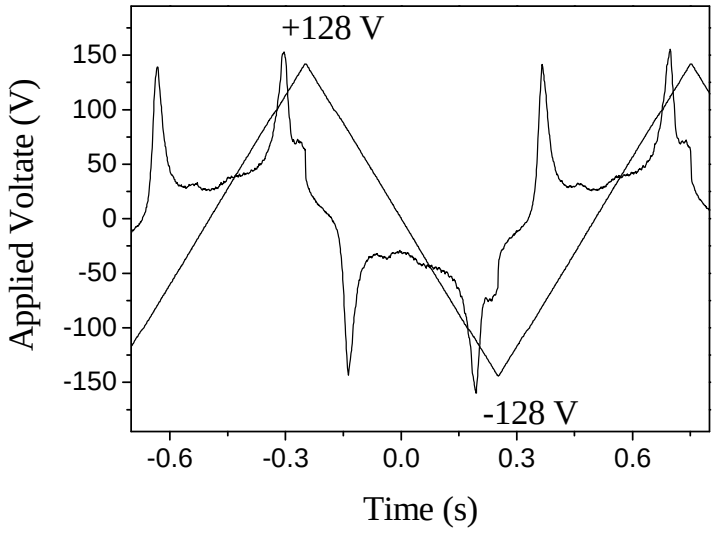

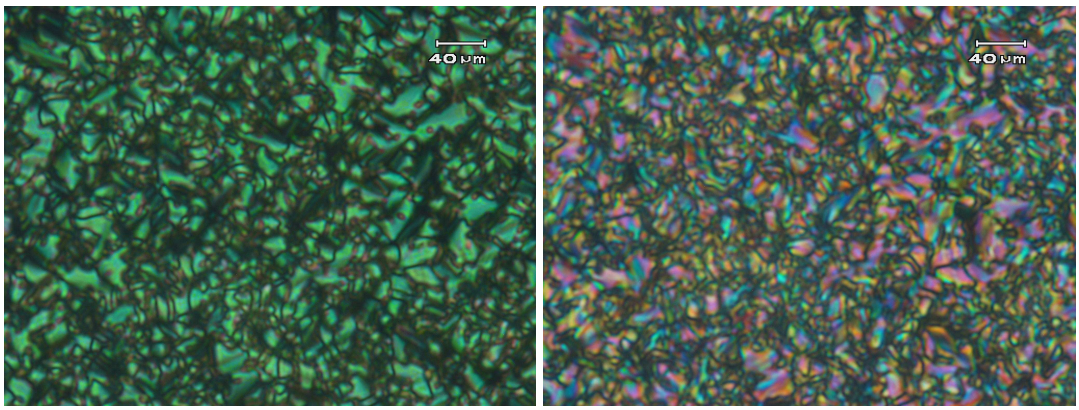

(b) **(c)**

Figure 6.12: (a) Switching current response trace obtained in the lower temperature SmC_sP_A phase of compound 6.A.10 on applying a triangular-wave electric field, at T = 94 °C; 4 Hz; 256 V_{pp}; $P_S \approx 375$ nC cm^{-2}. Photomicrographs obtained in the SmC_sP_A phase (b) under the electric field (c) without the electric field.

(a)

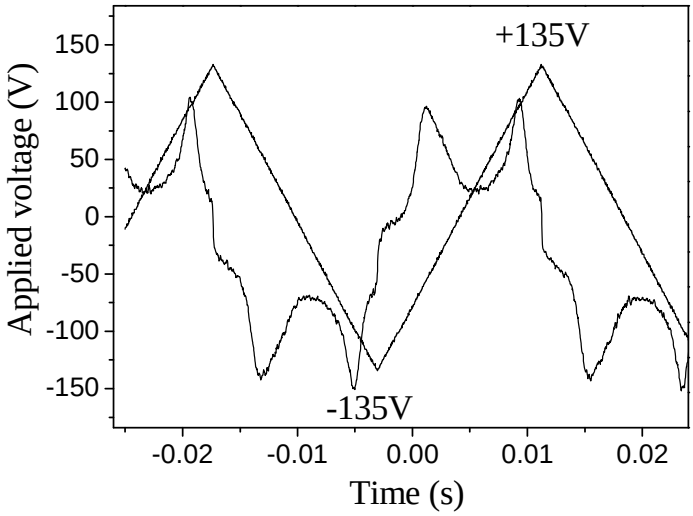

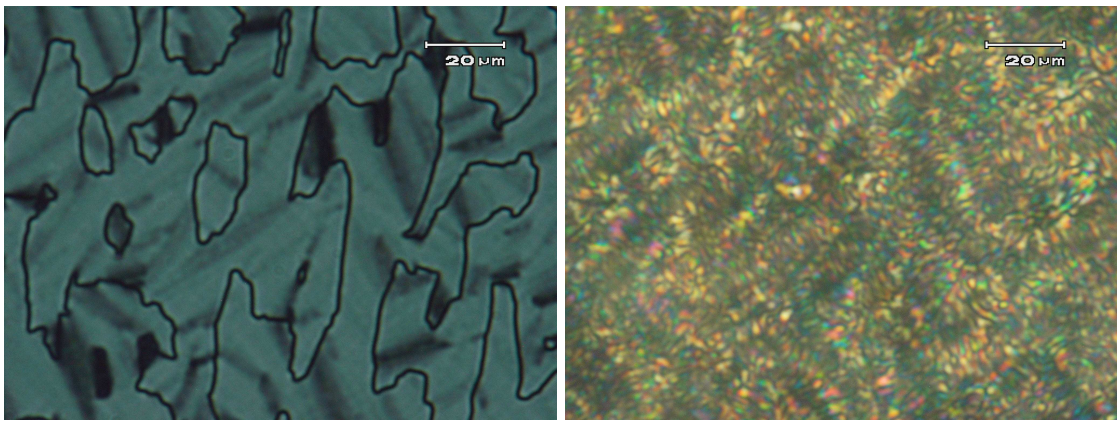

(b) **(c)**

Figure 6.13: (a) Switching current response trace obtained in the lowest temperature SmC'_sP_A phase of compound 6.A.10 on applying a triangular-wave electric field, at T = 84 °C; 35 Hz; 270 V_{pp}; $P_S \approx 385$ nC cm^{-2}. Photomicrographs obtained in the SmC'_sP_A phase (b) with field (c) without the electric field.

this confirmed again an antiferroelectric behaviour. The low birefringent texture observed under the field suggests an anticlinic arrangement in the layers and grainy texture is obtained if the field is removed. The switching current response obtained for the lowest temperature mesophase along with the optical textures are shown in figures **6.13.a, 6.13.b** and **6.13.c** respectively.

Further, dc field experiments were carried out for compound **6.A.10** in order to determine the ground state of smectic phases and the same cell was used for this purpose. Thus, smooth fan-shaped texture obtained on slow cooling from the nematic phase in the lower temperature mesophase is shown in figure **6.14.b**. In this, the dark brush is rotated by a small angle with respect to crossed polarizers indicating a synclinic arrangement and on applying a dc field upto ± 9.5 V μm^{-1}, there was no change in the position of the dark brushes suggesting that the switching takes place around the long axis under dc field. Thus, this suggests that a SmC_sP_A racemic structure goes to a polar SmC_sP_F phase. The optical textures obtained during the experiments are shown in figures **6.14.a, 6.14.b** and **6.14.c.** On further cooling into the lowest temperature phase, synclinic arrangement was observed. The rotation of the dark brush was observed clearly on application of dc field of 3 V μm^{-1} and textures obtained in the field on and field off states are shown in figures **6.15.a, 6.15.b** and **6.15.c.** This observation suggests that the molecules rotate around a cone and retains chirality under the field. Thus, the switching mechanisms of these two smectic phases are different.

The electro-optical switching behaviour suggests that both the smectic phases of compounds **6.A.9** and **6.A.10** are antiferroelectric with synclinic arrangement of the molecules. This type of phase sequence has been reported in the literature for dimers composed of bent-core and rod-like system [24] and it was observed that synclinic arrangement of the mesophases was not affected by electric field in both the cases. However, the switching mechanism is different for the lowest temperature mesophase of our compounds. Hence, we have characterized the mesophases as SmC_sP_A and SmC'_sP_A phases respectively. It should be noted that the behaviour of $SmCP_A$ phase of compounds **6.A.4, 6.A.5** and **6.A.6** seems to be similar to lowest temperature SmC'_sP_A phase of compounds **6.A.9** and **6.A.10** under field.

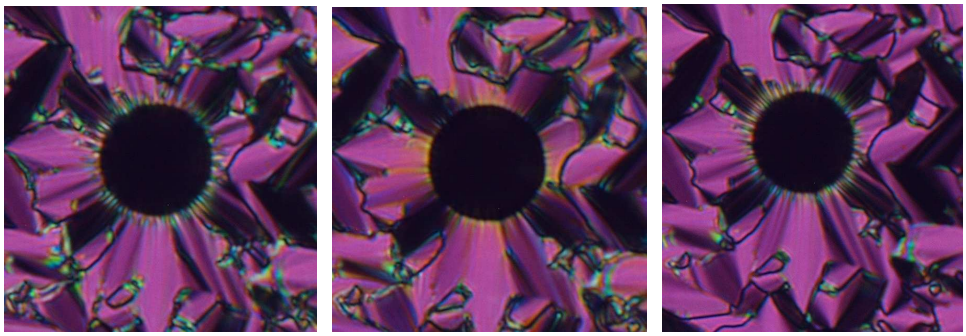

(a) (b) (c)

Figure 6.14: Photomicrographs obtained in the SmC_sP_A phase of compound 6.A.10 (a) + 9.5 V μm^{-1}; (b) 0 V and (c) - 9.5 V μm^{-1} under a dc electric field at T = 95 °C.

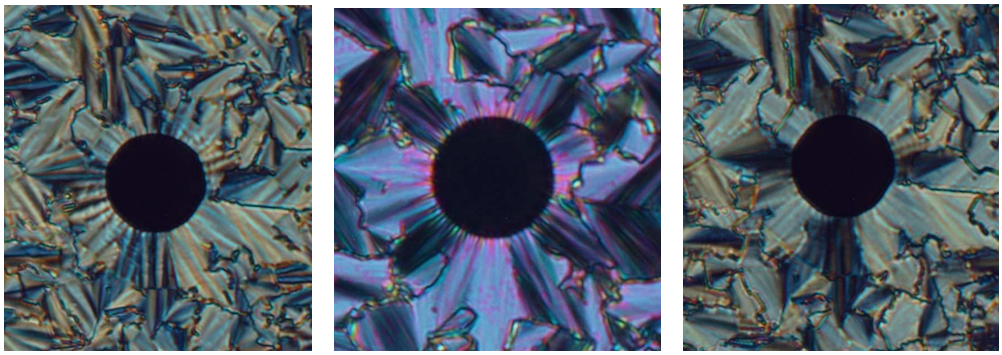

(a) (b) (c)

Figure 6.15: Photomicrographs obtained in the SmC'_sP_A phase of compound 6.A.10 (a) + 3 V μm^{-1}; (b) 0 V and (c) - 3 V μm^{-1} under a dc field at T = 84 °C.

6.3.5: Miscibility studies

In an effort to determine the structure of the two antiferroelectric mesophases of compounds **6.A.9** and **6.A.10** and also to overcome the problem of rapid crystallization of these pure compounds, we have prepared 50:50 mixture of compounds **6.A.8** and **6.A.10.** A DSC thermogram obtained for this mixture is shown in figure **6.16.** The melting point of the mixture was found to be 85 °C, which is about 10 °C less than those for pure compounds. As a result all the mesophases became enantiotropic and noticeably only three transitions were observed in DSC as well as under a polarizing microscope. The optical textures and electro-optical switching behaviour are similar to those obtained for pure compound **6.A.10.** The XRD measurements performed for powder sample in the higher temperature antiferroelectric phase at T = 89 °C showed only one reflection in the small angle region at d_1 = 45 Å whereas in the lower temperature antiferroelectric phase at T = 78 °C gave three reflections in the small angle region and d-spacings correspond to d_1 = 47 Å d_2 = 23.5 Å and d_3 = 15.6 Å. These reflections are in the ratio of 1 : ½ : ⅓ suggesting a lamellar ordering in the mesophase. The exposure time used for XRD measurements in both the mesophases was T = 30 min. The sample crystallizes on increasing the exposure time in the lowest temperature phase. On the basis of XRD measurements, the mesophases have been characterized as smectic phase and the possibility of this being a 2D columnar structure can be ruled out. The XRD intensity profile obtained in the mesophases for this mixture is shown in figure **6.17.**

6.3.6: Electro-convection pattern

It was observed that the nematic phase of compounds exhibit different types of pattern above a threshold voltage and as a function of frequency due to their hydrodynamic instability and these patterns are known as electro-convection patterns. These electro hydrodynamic instability is well understood in calamitic system. Wiant *et al.* [25] observed three types of instabilities in the nematic phase of compounds composed of bent-core molecules. Interestingly, electro-convection patterns were observed in the nematic phase of compounds of series **6.B** under field as a result of electrohydrodynamic instabilities. For example, when a sample of compound **6.B.3** was filled in a cell treated for planar alignment and cooled to nematic phase, the

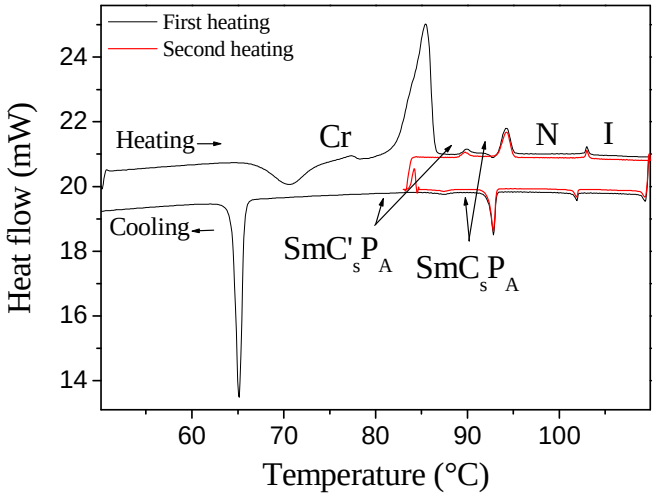

Figure 6.16: A DSC thermogram obtained for 50:50 mixture of compounds 6.A.8 and 6.A.10 showing all three enantiotropic phase transitions; scan rate 5 °C min^{-1}.

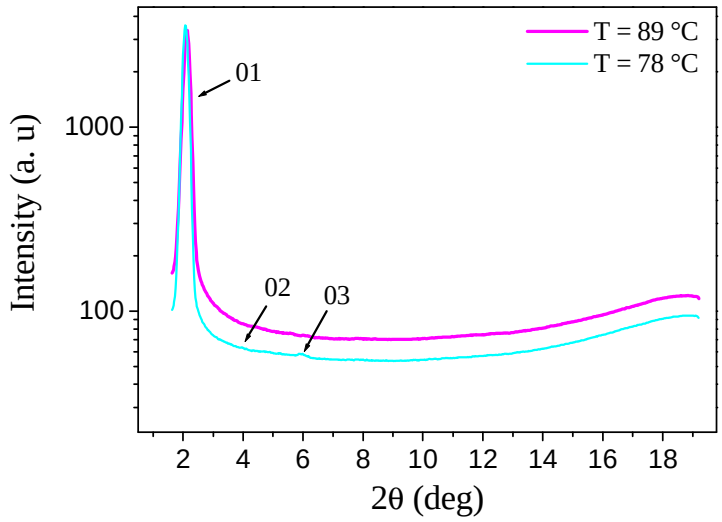

Figure 6.17: XRD intensity profile obtained for 50:50 mixture of compounds 6.A.8 and 6.A.10 in the SmC_sP_A (T = 89 °C) and SmC'_sP_A (T = 78 °C) mesophases.

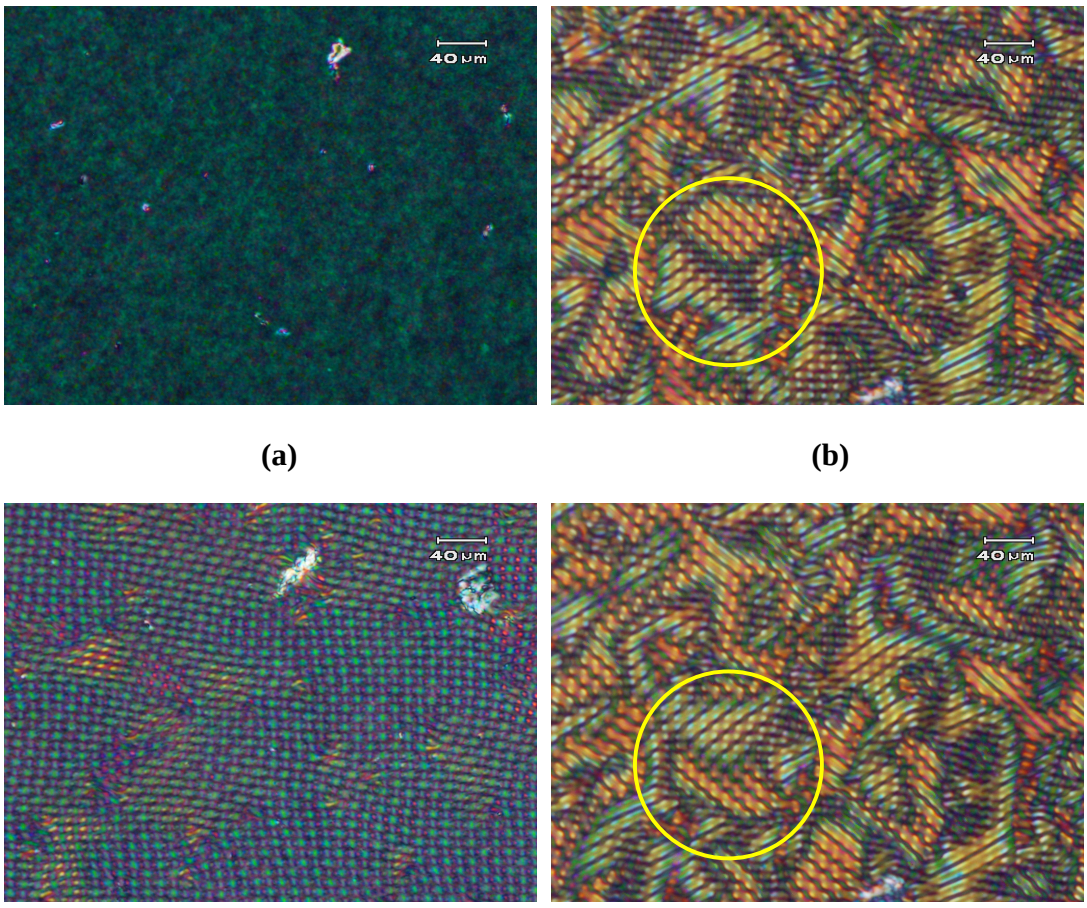

Figure 6.18: Photomicrographs of electro-convection patterns of compound 6.B.3 in a cell treated for planar alignment. (a) Nematic phase at T = 114 °C; (b) and (c) electro-convection patterns showing two opposite domains at T = 114 °C, 21 V_{pp} and 35 Hz; (d) uniform domain at T = 95 °C under the same conditions.

optical texture obtained is shown in figure **6.18.a.** On application of a voltage of 21 V_{pp} and a frequency of 35 Hz, electro-convection pattern was observed and these patterns are shown in figures **6.18.b** and **6.18.c**. It was observed that two different domains move in opposite directions continuously and this is shown in figures **6.18.b** and **6.18.c** by yellow circle. There was no change in the pattern on variation of frequency and the same pattern was observed over the entire thermal range of the mesophase. On further cooling, movement of domains was restricted and as a result a uniform pattern was obtained and this is shown in figure **6.18.d** which is close to crystallization temperature. Detailed physical experiments are necessary to understand the exact nature of these patterns and they are in progress.

6.4.1: Comparison between the mesophases of compounds of series 6.A and 6.B

It was found that all compounds belonging to both the series exhibited nematic phase. Interestingly, the nematic phase is enantiotropic in series **6.A** and is monotropic in series **6.B.** It can be clearly seen that compound **6.A.1** showed enantiotropic nematic phase in addition to Col_r phase while the corresponding analogue compound **6.B.4** exhibited enantiotropic nematic phase but with the same thermal range of 6 °C. On increasing the chain length from -OC_8 to -$OC_{16,}$ it was observed that the melting points decreased by 17 °C and also induced polar smectic phases in addition to nematic phase in series **6.A** whereas melting point increased by 3 °C in series **6.B**. However, the nematic phase got destabilized in methyl substituted compounds of series **6.B.** On increasing the chain length further, a polar smectic phase was induced and as a result compound **6.A.10** exhibited two polar smectic phases in addition to nematic phase. In series **6.B**, compounds **6.B.1** and **6.B.2** having shorter chain length of -OC_5 and -OC_6 induced non-polar SmC phase in addition to nematic phase. Although the size of chloro and methyl groups are comparable, the opposing polarity seems to influence the mesophases drastically. Compounds of series **6.A** contain a lateral chloro substituent which stabilizes the nematic phase as well as banana phases whereas compounds of series **6.B** containing a methyl substitutent destabilizes the nematic phase and also eliminates the banana phases.

6.4.2: Effect of chloro, methyl and fluoro lateral substituents

When compared to the fluoro substituted compounds, the analogous chloro substituted compounds have lower melting and clearing temperatures. While compound **6.A.9** shows two polar smectic phases in addition to a nematic phase, the fluoro analogue exhibits only a $SmCP_A$ phase. It is clear from our study that B-phases are stabilized by electronegative fluoro and chloro substituents while electropositive methyl substituent eliminates B-phases. Interestingly, all the laterally substituted compounds exhibit a nematic phase.

6.5: Conclusions

Two new series of bent-core compounds derived from 2,7-dihydroxynaphthalene containing a chloro or a methyl substituent on the middle phenyl rings in the side arms were synthesized and the influence of these groups on the mesophases were investigated. All compounds exhibit a nematic phase. Interestingly, compounds of series **6.A** containing a electronegative chloro lateral substituent showed rich polymorphism and thus three different phase sequences such as N→Col_r, N→$SmCP_A$ and N→SmC_sP_A→SmC'_sP_A phases were observed. Miscibility and XRD studies indicate that the two antiferroelectric mesophases are indeed lamellar and have been designated as SmC_sP_A and SmC'_sP_A. However, homologues of series **6.B** containing a electropositive methyl lateral substituent showed N→SmC and N phases. Although the size of the chloro and methyl groups are comparable the dipolar nature is different. Thus, chloro lateral substituent stabilizes the nematic as well as B-phases whereas methyl substituent eliminates B-phases. Electrohydro-dynamic instabilities were observed in the nematic phase of compounds of series **6.B**.

Experimental

3-Chloro-4-benzyloxybenzoic acid, 6.d (X = Cl)

3-Chloro-4-benzyloxybenzoic acid, **6.d** was prepared in three steps following the synthetic route shown in scheme **6.1.** This was prepared from 3-chloro-4-hydroxybenzoic acid, **6.a** by first refluxing in methanol and a catalytic amount of conc. sulphuric acid. Hydroxyl group of methyl 3-chloro-4-hydroxybenzoate, **6.b** was protected using benzyl chloride and anhydrous potassium carbonate in anhydrous butan-2-one. Thus, methyl 3-chloro-4-benzyloxybenzoate, **6.c** (8 g, 28 mmol) was hydrolyzed in ethanol (125 mL), potassium hydroxide (4.86 g, 86 mmol) and water by refluxing overnight. The excess of ethanol was distilled off, reaction mixture was cooled and poured into ice-cold water. The resulting solution was acidified with conc. HCl and heated on a water-bath for an hour and cooled. The white precipitate thus obtained was filtered off, washed several times with ice-cold water until the washings were neutral to litmus and dried. The material so obtained was crystallized using ethyl alcohol. Yield: 7.21 g (95%); mp 214.5-216 °C; IR (nujol) ν_{max}: 2952, 2923, 2854, 1681, 1596, 1566, 1506, 1456, 1377 cm^{-1}; ^1H NMR (400 MHz, CD_3COCD_3) δ: 8.02 (d, J = 2.07 Hz, 1H, Ar-H), 7.95 (dd, J_1 = 2.09 Hz, J_2 = 6.54 Hz, 1H, Ar-H), 7.53 (d, J = 7.54 Hz, 2H, Ar-H), 7.42 (t, J = 7.08 Hz, 2H, Ar-H), 7.37-7.31 (m, 2H, Ar-H), 5.33 (s, 2H, Ar-O-CH_2-); Elemental analysis: $C_{14}H_{11}ClO_3$ requires C 64.01, H 4.22; found C 63.78, H 4.44%.

3-Methyl-4-benzyloxybenzoic acid, 6.d (X = CH_3)

This was prepared following a procedure described in the literature [22].

E-4-*n*-alkoxy-α-methylcinnamic acids, 6.h

These acids were prepared according to the procedure described in the literature [23].

2,7-Naphthylene bis(3-chloro-4-benzyloxybenzoate), 6.f (X = Cl)

A mixture of 2,7-dihydroxynaphthalene, **6.e** (2 g, 12.5 mmol), 3-chloro-4-benzyloxybenzoic acid, **6.d** (6.8 g, 26.2 mmol) and a catalytic amount of 4-(*N*,*N*-dimethyl-amino)pyridine (DMAP) in dry chloroform (50 mL) was stirred for 10 min. To this mixture, *N*,*N'*-dicyclohexylcarbodiimide (DCC), (5.6 g, 27.7 mmol) was added and stirring continued for

24 h at room temperature. The precipitated *N*,*N*´-dicyclohexylurea was filtered off and washed with an excess of chloroform. Evaporation of the solvent from the filtrate gave a white material. This was further purified by column chromatography using chloroform as an eluant. The removal of the solvent followed by repeated crystallization using a mixture of alcohol and chloroform provided compound **6.f**. Yield: 7.5 g (92%); mp 183-185 °C; IR (nujol) ν_{max}: 2922, 2854, 1724, 1639, 1600, 1502, 1461, 1377 cm^{-1}; ^1H NMR (400 MHz, $CDCl_3$) δ: 8.28 (d, *J* = 2.12 Hz, 2H, Ar-H), 8.1 (dd, J_1 = 2.14 Hz, J_2 = 6.49 Hz, 2H, Ar-H), 7.92 (d, *J* = 8.98 Hz, 2H, Ar-H), 7.65 (d, *J* = 2.14 Hz, 2H, Ar-H), 7.49-7.32 (m, 12H, Ar-H), 7.07 (d, *J* = 8.72 Hz, 2H, Ar-H), 5.28 (s, 4H, 2 × Ar-O-CH_2-); Elemental analysis: $C_{38}H_{26}Cl_2O_6$ requires C 70.27, H 4.03; found C 69.87, H 3.97%.

2,7-Naphthylene bis(3-chloro-4-hydroxybenzoate), 6.g (X = Cl)

Compound, **6.f** (7 g) and 5% Pd-C catalyst (1.4 g) were taken in 1,4-dioxane (75 mL) and stirred in an atmosphere of hydrogen at 55 °C until the required quantity of hydrogen was absorbed. The resulting mixture was filtered hot and the solvent removed under reduced pressure. The material was crystallized using a mixture of 1,4-dioxane and petroleum ether (bp 60-80 ºC) to obtain pure compound **6.g.** Yield: 4.7 g (87%); mp 223-225 °C; IR (nujol) ν_{max}: 3344, 2923, 2852, 1730, 1703, 1598, 1583, 1512, 1454, 1375 cm^{-1}; ^1H NMR (400 MHz, CD_3COCD_3) δ: 9.9 (s, 2H, 2 × Ar-OH, exchangeable with D_2O), 8.18 (d, *J* = 2.05 Hz, 2H, Ar-H), 8.06-8.02 (m, 4H, Ar-H), 7.82 (d, *J* = 1.88 Hz, 2H, Ar-H), 7.46 (dd, J_1 = 2.11 Hz, J_2 = 6.68 Hz, 2H, Ar-H), 7.21 (d, *J* = 8.52 Hz, 2H, Ar-H); Elemental analysis: $C_{24}H_{14}Cl_2O_6$ requires C 61.42, H 3; found C 61.83, H 2.91%.

2,7-Naphthylene bis(3-methyl-4-benzyloxybenzoate), 6.f (X = Me)

This was synthesized following a procedure described for the preparation of compound **6.f,** by using 2,7-dihydroxynaphthalene, **6.e** and 3-methyl-4-benzyloxybenzoic acid, **6.d** in dry dichloromethane. Yield: (94%); mp 176.5-178 °C; IR (nujol) ν_{max}: 2952, 2923, 2854, 1724, 1639, 1606, 1581, 1504, 1444, 1417, 1377 cm^{-1}; ^1H NMR (400 MHz, $CDCl_3$) δ: 8.11-8.06 (m, 3H, Ar-H), 7.91 (d, *J* = 8.89 Hz, 2H, Ar-H), 7.65 (d, *J* = 1.94 Hz, 2H, Ar-H), 7.51-7.33 (m, 12H, Ar-H), 6.98 (d, *J* = 8.39 Hz, 2H, Ar-H), 5.20 (s, 4H, 2 × Ar-O-CH_2-), 2.36 (s, 6H, 2 × Ar-CH_3); Elemental analysis: $C_{40}H_{32}O_6$ requires C 78.93, H 5.29; found C 78.92, H 5.45%.

2,7-Naphthylene bis(3-methyl-4-hydroxybenzoate), 6.g (X = Me)

This was synthesized following a procedure described for the synthesis of compound **6.g,** by using compound **6.f** as starting material. Yield: (93%); mp 254.5-256.5 °C; IR (nujol) ν_{max}: 3396, 2952, 2923, 2854, 1710, 1697, 1596, 1508, 1458, 1375 cm^{-1}; ^1H NMR (400 MHz, DMSO-d_6) δ: 9.26 (s, 2H, 2 × Ar-OH, exchangeable with D_2O), 8.03 (d, *J* = 8.94 Hz, 2H, Ar-H), 7.98 (s, 2H, Ar-H), 7.93 (d, *J* = 8.4 Hz, 2H, Ar-H), 7.76 (d, *J* = 1.58 Hz, 2H, Ar-H), 7.43 (dd, J_1 = 2.07 Hz, J_2 = 6.83 Hz, 2H, Ar-H), 7 (d, *J* = 8.39 Hz, 2H, Ar-H), 2.4 (s, 6H, 2 × Ar-CH_3); Elemental analysis: $C_{26}H_{20}O_6$ requires C 72.89, H 4.7; found C 72.99, H 5%.

2,7-Naphthylene bis(4-(E-4-*n*-octyloxy-α-methylcinnamoyloxy)-3-chlorobenzoate), 6.A.1

A mixture of compound, **6.g** (0.2 g, 4.27 mmol), E-4-*n*-octyloxy-α-methylcinnamic acid, **6.h** (0.260 g, 8.97 mmol) and DCC (0.193 g, 9.39 mmol) in the presence of a catalytic amount of DMAP was stirred in dry dichloromethane for 24 h. The precipitated *N*,*N*´-dicyclohexylurea was filtered off and washed with an excess of chloroform. Evaporation of the solvent from the filtrate gave a material which was purified by passing through a column of silica gel using chloroform as an eluent. Removal of the solvent gave a white material. This material was further purified by repeated crystallization using a mixture of chloroform and acetonitrile. Yield: 0.250 g (58%); mp 113.5 °C; IR (KBr) ν_{max}: 3058, 2922, 2852, 1739, 1732, 1627, 1604, 1512, 1488, 1473, 1396 cm^{-1}; ^1H NMR (400 MHz, $CDCl_3$) δ: 8.38 (d, *J* = 1.92 Hz, 2H, Ar-H), 8.21 (dd, J_1 = 1.96 Hz, J_2 = 6.41 Hz, 2H, Ar-H), 7.98-7.95 (m, 2H, Ar-H), 7.99-7.97 (m, 2H, Ar-H), 7.96 (s, 2H, 2 × Ar-C<u>H</u>=C(CH_3)-), 7.71 (d, *J* = 1.58 Hz, 2H, Ar-H), 7.49 (d, *J* = 8.8 Hz, 2H, Ar-H), 7.43 (d, *J* = 8.66 Hz, 2H, Ar-H), 7.38 (dd, J_1 = 2.1 Hz, J_2 = 6.86 Hz, 2H, Ar-H), 6.96 (d, *J* = 8.6 Hz, 4H, Ar-H), 4.02 (t, *J* = 6.42 Hz, 4H, 2 × Ar-O-CH_2-), 2.31 (d, 6H, 2 × -CH=C(C<u>H</u>$_3$)COO-), 1.84-1.78 (quin, *J* = 6.45 Hz, 4H, 2 × Ar-O-CH_2-C<u>H</u>$_2$-), 1.52-1.28 (m, 20H, 2 × -$(CH_2)_5$-), 0.89 (t, *J* = 6.81 Hz, 6H, 2 × -CH_3); Elemental analysis: $C_{60}H_{62}Cl_2O_{10}$ requires C 71.07, H 6.16; found C 71.32, H 6.25%.

2,7-Naphthylene bis(4-(E-4-*n*-nonyloxy-α-methylcinnamoyloxy)-3-chlorobenzoate), 6.A.2

This compound and other homologues of series **6.A** and **6.B** were synthesized following a procedure described for the preparation of compound **6.A.1.**

Yield: (60%); mp 105 °C; IR (KBr) ν_{max}: 3057, 2922, 2852, 1735, 1730, 1627, 1604, 1595, 1504, 1488, 1373, 1398 cm^{-1}; ^1H NMR (400 MHz, $CDCl_3$) δ: 8.38 (d, *J* = 2 Hz, 2H, Ar-H), 8.21 (dd, J_1 = 2.12 Hz, J_2 = 6.46 Hz, 2H, Ar-H), 7.97-7.96 (m, 2H, Ar-H), 7.94 (s, 2H, 2 × Ar-C<u>H</u>=C(CH_3)-), 7.71 (d, *J* = 1.62 Hz, 2H, Ar-H), 7.48 (d, *J* = 8.86 Hz, 4H, Ar-H), 7.43 (d, *J* = 8.6 Hz, 2H, Ar-H), 7.37 (dd, J_1 = 2.02 Hz, J_2 = 6.63 Hz, 2H, Ar-H), 6.96 (d, *J* = 8.78 Hz, 4H, Ar-H), 4.01 (t, *J* = 6.52 Hz, 4H, 2 × Ar-O-CH_2-), 2.31 (d, 6H, 2 × -CH=C(C<u>H</u>$_3$)COO-), 1.84-1.77 (quin, *J* = 6.66 Hz, 4H, 2 × Ar-O-CH_2-C<u>H</u>$_2$-), 1.51-1.24 (m, 24H, 2 × -$(CH_2)_6$-), 0.89 (t, *J* = 6.64 Hz, 6H, 2 × -CH_3); Elemental analysis: $C_{62}H_{66}Cl_2O_{10}$ requires C 71.46, H 6.38; found C 71.79, H 6.13%.

2,7-Naphthylene bis(4-(E-4-*n*-decyloxy-α-methylcinnamoyloxy)-3-chlorobenzoate), 6.A.3

Yield: (61%); mp 96.5 °C; IR (KBr) ν_{max}: 3058, 2920, 2851, 1735, 1730, 1626, 1604, 1510, 1488, 1473, 1396 cm^{-1}; ^1H NMR (400 MHz, $CDCl_3$) δ: 8.38 (d, *J* = 1.87 Hz, 2H, Ar-H), 8.21 (dd, J_1 = 1.86 Hz, J_2 = 6.52 Hz, 2H, Ar-H), 7.99-7.97 (m, 2H, Ar-H), 7.95 (s, 2H, 2 × Ar-C<u>H</u>=C(CH_3)-), 7.7 (d, *J* = 1.62 Hz, 2H, Ar-H), 7.49 (d, *J* = 8.69 Hz, 4H, Ar-H), 7.43 (d, *J* = 8.45 Hz, 2H, Ar-H), 7.37 (dd, J_1 = 2.02 Hz, J_2 = 6.83 Hz, 2H, Ar-H), 6.96 (d, *J* = 8.69 Hz, 4H, Ar-H), 4.01 (t, *J* = 6.52 Hz, 4H, 2 × Ar-O-CH_2-), 2.31 (d, 6H, 2 × -CH=C(C<u>H</u>$_3$)COO-), 1.83-1.79 (quin, *J* = 7.01 Hz, 4H, 2 × Ar-O-CH_2-C<u>H</u>$_2$-), 1.56-1.28 (m, 28H, 2 × -$(CH_2)_7$-), 0.88 (t, *J* = 6.93 Hz, 6H, 2 × -CH_3); Elemental analysis: $C_{64}H_{70}Cl_2O_{10}$ requires C 71.83, H 6.59; found C 71.51, H 6.78%.

2,7-Naphthylene bis(4-(E-4-*n*-undecyloxy-α-methylcinnamoyloxy)-3-chlorobenzoate), 6.A.4

Yield: (59%); mp 96 °C; IR (KBr) ν_{max}: 3059, 2922, 2852, 1745, 1730, 1629, 1606, 1508, 1456, 1375 cm^{-1}; ^1H NMR (400 MHz, $CDCl_3$) δ: 8.38 (d, *J* = 1.98 Hz, 2H, Ar-H), 8.22 (dd, J_1 = 2.02 Hz, J_2 = 6.46 Hz, 2H, Ar-H), 7.97-7.96 (m, 2H, Ar-H), 7.94 (s, 2H, 2 × Ar-C<u>H</u>=C(CH_3)-), 7.7 (d, *J* = 1.88 Hz, 2H, Ar-H), 7.49 (d, *J* = 8.72 Hz, 4H, Ar-H), 7.43 (d, *J* = 8.56 Hz, 2H, Ar-H), 7.37 (dd, J_1 = 2.08 Hz, J_2 = 6.92 Hz, 2H, Ar-H), 6.96 (d, *J* = 8.78 Hz, 4H, Ar-H), 4.01 (t, *J* = 6.56 Hz, 4H, 2 × Ar-O-CH_2-), 2.31 (d, 6H, 2 × -CH=C(C<u>H</u>$_3$)COO-), 1.84-1.77 (quin, *J* = 7.04 Hz, 4H, 2 × Ar-O-CH_2-C<u>H</u>$_2$-), 1.54-1.26 (m, 32H, 2 × -$(CH_2)_8$-), 0.88 (t, *J* = 6.86 Hz, 6H, 2 × -CH_3); Elemental analysis: $C_{66}H_{74}Cl_2O_{10}$ requires C 72.18, H 6.79; found C 72.24, H 6.89%.

2,7-Naphthylene bis(4-(E-4-*n*-dodecyloxy-α-methylcinnamoyloxy)-3-chlorobenzoate), 6.A.5

Yield: (62%); mp 98.5 °C; IR (KBr) ν_{max}: 3056, 2922, 2852, 1745, 1730, 1631, 1604, 1595, 1510, 1461, 1377 cm^{-1}; ^1H NMR (400 MHz, $CDCl_3$) δ: 8.38 (d, *J* = 2.02 Hz, 2H, Ar-H), 8.22 (dd, J_1 = 2.04 Hz, J_2 = 6.46 Hz, 2H, Ar-H), 7.97-7.96 (m, 2H, Ar-H), 7.94 (s, 2H, 2 × Ar-C<u>H</u>=C(CH_3)-), 7.7 (d, *J* = 2.04 Hz, 2H, Ar-H), 7.48 (d, *J* = 8.8 Hz, 4H, Ar-H), 7.43 (d, *J* = 8.62 Hz, 2H, Ar-H), 7.37 (dd, J_1 = 2.12 Hz, J_2 = 6.86 Hz, 2H, Ar-H), 6.96 (d, *J* = 8.82 Hz, 4H, Ar-H), 4.01 (t, *J* = 6.58 Hz, 4H, 2 × Ar-O-CH_2-), 2.31 (d, 6H, 2 × -CH=C(C<u>H</u>$_3$)COO-), 1.84-1.77 (quin, *J* = 6.86 Hz, 4H, 2 × Ar-O-CH_2-C<u>H</u>$_2$-), 1.54-1.24 (m, 36H, 2 × -$(CH_2)_9$-), 0.88 (t, *J* = 6.96 Hz, 6H, 2 × -CH_3); Elemental analysis: $C_{68}H_{78}Cl_2O_{10}$ requires C 72.52, H 6.98; found C 72.88, H 7.29%.

2,7-Naphthylene bis(4-(E-4-*n*-tridecyloxy-α-methylcinnamoyloxy)-3-chlorobenzoate), 6.A.6

Yield: (61%); mp 94 °C; IR (KBr) ν_{max}: 3056, 2922, 2852, 1739, 1732, 1626, 1652, 1541, 1508, 1456, 1377 cm^{-1}; ^1H NMR (400 MHz, $CDCl_3$) δ: 8.38 (d, *J* = 2.04 Hz, 2H, Ar-H), 8.22 (dd, J_1 = 2.06 Hz, J_2 = 6.41 Hz, 2H, Ar-H), 7.97-7.96 (m, 2H, Ar-H), 7.94 (s, 2H, 2 × Ar-C<u>H</u>=C(CH_3)-), 7.7 (d, *J* = 2.06 Hz, 2H, Ar-H), 7.49 (d, *J* = 8.96 Hz, 4H, Ar-H), 7.43 (d, *J* = 8.46 Hz, 2H, Ar-H), 7.37 (dd, J_1 = 2.15 Hz, J_2 = 6.6 Hz, 2H, Ar-H), 6.96 (d, *J* = 8.8 Hz, 4H, Ar-H), 4.01 (t, *J* = 6.72 Hz, 4H, 2 × Ar-O-CH_2-), 2.31 (d, 6H, 2 × -CH=C(C<u>H</u>$_3$)COO-), 1.84-1.77 (quin, *J* = 6.9 Hz, 4H, 2 × Ar-O-CH_2-C<u>H</u>$_2$-), 1.54-1.26 (m, 40H, 2 × -$(CH_2)_{10}$-), 0.88 (t, *J* = 6.94 Hz, 6H, 2 × -CH_3); Elemental analysis: $C_{70}H_{82}Cl_2O_{10}$ requires C 72.84, H 7.16; found C 73.27, H 6.75%.

2,7-Naphthylene bis(4-(E-4-*n*-tetradecyloxy-α-methylcinnamoyloxy)-3-chlorobenzoate), 6.A.7

Yield: (58%); mp 94 °C; IR (KBr) ν_{max}: 3058, 2918, 2850, 1743, 1732, 1629, 1604, 1577, 1510, 1488, 1473, 1396 cm^{-1}; ^1H NMR (400 MHz, $CDCl_3$) δ: 8.37 (d, *J* = 2.02 Hz, 2H, Ar-H), 8.21 (dd, J_1 = 2.04 Hz, J_2 = 6.41 Hz, 2H, Ar-H), 7.97-7.96 (m, 2H, Ar-H), 7.94 (s, 2H, 2 × Ar-C<u>H</u>=C(CH_3)-), 7.7 (d, *J* = 2.08 Hz, 2H, Ar-H), 7.48 (d, *J* = 8.77 Hz, 4H, Ar-H), 7.43 (d, *J* = 8.46 Hz, 2H, Ar-H), 7.37 (dd, J_1 = 2.19 Hz, J_2 = 6.63 Hz, 2H, Ar-H), 6.96 (d, *J* = 8.78 Hz, 4H, Ar-H), 4.01 (t, *J* = 6.52 Hz, 4H, 2 × Ar-O-CH_2-), 2.3 (d, 6H, 2 × -CH=C(C<u>H</u>$_3$)COO-), 1.84-1.77 (quin, *J* = 6.65 Hz, 4H, 2 × Ar-O-CH_2-C<u>H</u>$_2$-), 1.51-1.24 (m, 44H, 2 × -$(CH_2)_{11}$-), 0.88 (t,

J = 6.6 Hz, 6H, 2 × -CH_3); Elemental analysis: $C_{72}H_{86}Cl_2O_{10}$ requires C 73.14, H 7.34; found C 73.59, H 7.61%.

2,7-Naphthylene bis(4-(E-4-*n*-pentadecyloxy-α-methylcinnamoyloxy)-3chlorobenzoate), 6.A.8

Yield: (58%); mp 97 °C; IR (KBr) ν_{max}: 3056, 2922, 2852, 1737, 1732, 1693, 1629, 1598, 1510, 1454, 1377 cm^{-1}; ^1H NMR (400 MHz, $CDCl_3$) δ: 8.38 (d, *J* = 2.03 Hz, 2H, Ar-H), 8.22 (dd, J_1 = 2 Hz, J_2 = 3.14 Hz, 2H, Ar-H), 7.98-7.96 (m, 2H, Ar-H), 7.94 (s, 2H, 2 × Ar-C<u>H</u>=C(CH_3)-), 7.71 (d, *J* = 2.07 Hz, 2H, Ar-H), 7.49 (d, *J* = 8.77 Hz, 4H, Ar-H), 7.43 (d, *J* = 8.46 Hz, 2H, Ar-H), 7.38 (dd, J_1 = 2.2 Hz, J_2 = 6.6 Hz, 2H, Ar-H), 6.96 (d, *J* = 8.78 Hz, 4H, Ar-H), 4.01 (t, *J* = 6.6 Hz, 4H, 2 × Ar-O-CH_2-), 2.31 (d, 6H, 2 × -CH=C(C<u>H</u>$_3$)COO-), 1.84-1.77 (quin, *J* = 6.7 Hz, 4H, 2 × Ar-O-CH_2-C<u>H</u>$_2$-), 1.55-1.26 (m, 48H, 2 × -$(CH_2)_{12}$-), 0.88 (t, *J* = 6.6 Hz, 6H, 2 × -CH_3); Elemental analysis: $C_{74}H_{90}Cl_2O_{10}$ requires C 73.43, H 7.48; found C 73.62, H 7.62%.

2,7-Naphthylene bis(4-(E-4-*n*-hexadecyloxy-α-methylcinnamoyloxy)-3-chlorobenzoate), 6.A.9

Yield: (60%); mp 96.5 °C; IR (KBr) ν_{max}: 3058, 2922, 2852, 1745, 1730, 1631, 1604, 1595, 1508, 1461, 1377 cm^{-1}; ^1H NMR (400 MHz, $CDCl_3$) δ: 8.38 (d, *J* = 2 Hz, 2H, Ar-H), 8.22 (dd, J_1 = 2.04 Hz, J_2 = 6.41 Hz, 2H, Ar-H), 7.99-7.96 (m, 2H, Ar-H), 7.95 (s, 2H, 2 × Ar-C<u>H</u>=C(CH_3)-), 7.7 (d, *J* = 2 Hz, 2H, Ar-H), 7.49 (d, *J* = 8.74 Hz, 4H, Ar-H), 7.43 (d, *J* = 8.46 Hz, 2H, Ar-H), 7.38 (dd, J_1 = 2.16 Hz, J_2 = 6.6 Hz, 2H, Ar-H), 6.96 (d, *J* = 8.76 Hz, 4H, Ar-H), 4.01 (t, *J* = 6.5 Hz, 4H, 2 × Ar-O-CH_2-), 2.31 (d, 6H, 2 × -CH=C(C<u>H</u>$_3$)COO-), 1.84-1.77 (quin, *J* = 6.56 Hz, 4H, 2 × Ar-O-CH_2-C<u>H</u>$_2$-), 1.55-1.26 (m, 52H, 2 × -$(CH_2)_{13}$-), 0.88 (t, *J* = 6.8 Hz, 6H, 2 × -CH_3); Elemental analysis: $C_{76}H_{94}Cl_2O_{10}$ requires C 73.71, H 7.65; found C 74.04, H 8.07%.

2,7-Naphthylene bis(4-(E-4-*n*-octadecyloxy-α-methylcinnamoyloxy)-3-chlorobenzoate), 6.A.10

Yield: (58%); mp 95.5 °C; IR (KBr) ν_{max}: 3060, 2918, 2850, 1747, 1732, 1627, 1604, 1510, 1488, 1473, 1396 cm^{-1}; ^1H NMR (400 MHz, $CDCl_3$) δ: 8.38 (d, *J* = 2.02 Hz, 2H, Ar-H),

8.21 (dd, J_1 = 2 Hz, J_2 = 6.6 Hz, 2H, Ar-H), 7.97-7.96 (m, 2H, Ar-H), 7.94 (s, 2H, 2 × Ar-C<u>H</u>=C(CH_3)-), 7.7 (d, J = 2 Hz, 2H, Ar-H), 7.49 (d, J = 8.76 Hz, 4H, Ar-H), 7.43 (d, J = 8.47 Hz, 2H, Ar-H), 7.37 (dd, J_1 = 2.1 Hz, J_2 = 6.7 Hz, 2H, Ar-H), 6.96 (d, J = 8.77 Hz, 4H, Ar-H), 4.01 (t, J = 6.5 Hz, 4H, 2 × Ar-O-CH_2-), 2.31 (d, 6H, 2 × -CH=C(C<u>H</u>$_3$)COO-), 1.84-1.77 (quin, J = 6.59 Hz, 4H, 2 × Ar-O-CH_2-C<u>H</u>$_2$-), 1.55-1.26 (m, 60H, 2 × -$(CH_2)_{15}$-), 0.88 (t, J = 6.55 Hz, 6H, 2 × -CH_3); Elemental analysis: $C_{80}H_{102}Cl_2O_{10}$ requires C 74.22, H 7.94; found C 73.87, H 8.3%.

2,7-Naphthylene bis(4-(E-4-*n*-pentyloxy-α-methylcinnamoyloxy)-3-methylbenzoate), 6.B.1

Yield: (60%); mp 138.5 °C; IR (KBr) ν_{max}: 3060, 2923, 2854, 1730, 1701, 1627, 1604, 1504, 1456, 1377 cm^{-1}; ^{1}H NMR (400 MHz, $CDCl_3$) δ: 8.18-8.13 (m, 4H, Ar-H), 7.95-7.93 (m, 4H, Ar-H), 7.68 (d, J = 1.81 Hz, 2H, Ar-H), 7.48 (d, J = 8.69 Hz, 4H, Ar-H), 7.37 (dd, J_1 = 2.1 Hz, J_2 = 6.79 Hz, 2H, Ar-H), 7.29-7.27 (m, 2H, Ar-H), 6.96 (d, J = 8.71 Hz, 4H, Ar-H), 4.01 (t, J = 6.55 Hz, 4H, 2 × Ar-O-CH_2-), 2.34 (s, 6H, 2 × -Ar-CH_3), 2.3 (d, 6H, 2 × -CH=C(C<u>H</u>$_3$)COO-), 1.85-1.78 (quin, J = 6.59 Hz, 4H, 2 × Ar-O-CH_2-C<u>H</u>$_2$-), 1.5-1.37 (m, 8H, 2 × -$(CH_2)_2$-), 0.94 (t, J = 7.1 Hz, 6H, 2 ×-CH_3); Elemental analysis: $C_{56}H_{56}O_{10}$ requires C 75.65, H 6.35; found C 75.8, H 6.62%.

2,7-Naphthylene bis(4-(E-4-*n*-hexyloxy-α-methylcinnamoyloxy)-3-methylbenzoate), 6.B.2

Yield: (62%); mp 120 °C; IR (KBr) ν_{max}: 3056, 2923, 2852, 1718, 1627, 1604, 1504, 1454, 1377 cm^{-1}; ^{1}H NMR (400 MHz, $CDCl_3$) δ: 8.18-8.13 (m, 4H, Ar-H), 7.96-7.93 (m, 4H, Ar-H), 7.69 (d, J = 1.81 Hz, 2H, Ar-H), 7.47 (d, J = 8.66 Hz, 4H, Ar-H), 7.37 (dd, J_1 = 2.07 Hz, J_2 = 6.74 Hz, 2H, Ar-H), 7.29-7.27 (m, 2H, Ar-H), 6.96 (d, 4H, J = 8.7 Hz, 4H, Ar-H), 4.01 (t, J = 6.51 Hz, 4H, 2 × Ar-O-CH_2-), 2.33 (s, 6H, 2 × -Ar-CH_3), 2.3 (d, 6H, 2 × -CH=C(C<u>H</u>$_3$)COO-), 1.84-1.77 (quin, J = 6.7 Hz, 4H, 2 × Ar-O-CH_2-C<u>H</u>$_2$-), 1.49-1.35 (m, 12H, 2 × -$(CH_2)_3$-), 0.91 (t, J = 6.91 Hz, 6H, 2 × -CH_3); Elemental analysis: $C_{58}H_{60}O_{10}$ requires C 75.96, H 6.59; found C 75.58, H 6.72%.

2,7-Naphthylene bis(4-(E-4-*n*-heptyloxy-α-methylcinnamoyloxy)-3-methylbenzoate), 6.B.3

Yield: (60%); mp 112.5 °C; IR (KBr) ν_{max}: 3057, 2954, 2922, 2852, 1726, 1629, 1604, 1514, 1454, 1377 cm^{-1}; ^{1}H NMR (400 MHz, $CDCl_3$) δ: 8.19-8.14 (m, 4H, Ar-H), 7.96-7.93 (m,

4H, Ar-H), 7.69 (d, *J* = 2.2 Hz, 2H, Ar-H), 7.48 (d, *J* = 8.8 Hz, 4H, Ar-H), 7.38 (dd, J_1 = 2.24 Hz, J_2 = 6.65 Hz, 2H, Ar-H), 7.29-7.27 (m, 2H, Ar-H), 6.97 (d, *J* = 8.8 Hz, 4H, Ar-H), 4.01 (t, *J* = 6.57 Hz, 4H, 2 × Ar-O-CH_2-), 2.34 (s, 6H, 2 × -Ar-CH_3), 2.27 (d, 6H, 2 × -CH=C(C$\underline{H}_3$)COO-), 1.85-1.77 (quin, *J* = 6.92 Hz, 4H, 2 × Ar-O-CH_2-C$\underline{H}_2$-), 1.51-1.29 (m, 16H, 2 × -$(CH_2)_4$-), 0.9 (t, *J* = 6.76 Hz, 6H, 2 × -CH_3); Elemental analysis: $C_{60}H_{64}O_{10}$ requires C 76.25, H 6.82; found C 76.07, H 6.94%.

2,7-Naphthylene bis(4-(E-4-*n*-octyloxy-α-methylcinnamoyloxy)-3-methylbenzoate), 6.B.4

Yield: (61%); mp 113.5 °C; IR (KBr) ν_{max}: 3056, 2954, 2920, 2850, 1726, 1631, 1604, 1504, 1454, 1377 cm^{-1}; ^{1}H NMR (400 MHz, $CDCl_3$) δ: 8.18-8.13 (m, 4H, Ar-H), 7.95-7.93 (m, 4H, Ar-H), 7.69 (d, *J* = 2.18 Hz, 2H, Ar-H), 7.47 (d, *J* = 8.96 Hz, 4H, Ar-H), 7.37 (dd, J_1 = 2.2 Hz, J_2 = 6.68 Hz, 2H, Ar-H), 7.29-7.27 (m, 2H, Ar-H), 6.96 (d, *J* = 8.76 Hz, 4H, Ar-H), 4.01 (t, *J* = 6.6 Hz, 4H, 2 × Ar-O-CH_2-), 2.34 (s, 6H, 2 × -Ar-CH_3), 2.3 (d, 6H, 2 × -CH=C(C$\underline{H}_3$)COO-), 1.83-1.79 (quin, *J* = 6.8 Hz, 4H, 2 × Ar-O-CH_2-C$\underline{H}_2$-), 1.53-1.3 (m, 20H, 2 × -$(CH_2)_5$-), 0.89 (t, *J* = 6.76 Hz, 6H, 2 × -CH_3); Elemental analysis: $C_{62}H_{68}O_{10}$ requires C 76.52, H 7.04; found C 76.81, H 7.25%.

2,7-Naphthylene bis(4-(E-4-*n*-nonyloxy-α-methylcinnamoyloxy)-3-methylbenzoate), 6.B.5

Yield: (59%); mp 112.5 °C; IR (KBr) ν_{max}: 3058, 2954, 2921, 2852, 1730, 1727, 1627, 1606, 1508, 1456, 1375 cm^{-1}; ^{1}H NMR (400 MHz, $CDCl_3$) δ: 8.18-8.14 (m, 4H, Ar-H), 7.96-7.94 (m, 4H, Ar-H), 7.69 (d, *J* = 2.16 Hz, 2H, Ar-H), 7.48 (d, *J* = 8.8 Hz, 4H, Ar-H), 7.38 (dd, J_1 = 2.2 Hz, J_2 = 6.65 Hz, 2H, Ar-H), 7.29-7.27 (m, 2H, Ar-H), 6.97 (d, *J* = 8.8 Hz, 4H, Ar-H), 4.01 (t, *J* = 6.6 Hz, 4H, 2 × Ar-O-CH_2-), 2.34 (s, 6H, 2 × -Ar-CH_3), 2.3 (d, 6H, 2 × -CH=C(C$\underline{H}_3$)COO-), 1.84-1.77 (quin, *J* = 6.92 Hz, 4H, 2 × Ar-O-CH_2-C$\underline{H}_2$-), 1.51-1.29 (m, 24H, 2 × -$(CH_2)_6$-), 0.89 (t, *J* = 6.72 Hz, 6H, 2 × -CH_3); Elemental analysis: $C_{64}H_{72}O_{10}$ requires C 76.77, H 7.25; found C 77.07, H 7.43%.

2,7-Naphthylene bis(4-(E-4-*n*-decyloxy-α-methylcinnamoyloxy)-3-methylbenzoate), 6.B.6

Yield: (60%); mp 111 °C; IR (KBr) ν_{max}: 3057, 2952, 2923, 2852, 1730, 1725, 1628, 1606, 1504, 1456, 1377 cm^{-1}; ^{1}H NMR (400 MHz, $CDCl_3$) δ: 8.17-8.12 (m, 4H, Ar-H), 7.94-7.92 (m, 4H, Ar-H), 7.68 (d, *J* = 1.9 Hz, 2H, Ar-H), 7.47 (d, *J* = 8.69 Hz, 4H, Ar-H), 7.37 (dd, J_1 = 2

Hz, J_2 = 6.78 Hz, 2H, Ar-H), 7.29-7.27 (m, 2H, Ar-H), 6.96 (d, J = 8.7 Hz, 4H, Ar-H), 4 (t, J = 6.47 Hz, 4H, 2 × Ar-O-CH_2-), 2.32 (s, 6H, 2 × -Ar-CH_3), 2.29 (d, 6H, 2 × -CH=C(C$\underline{H}_3$)COO-), 1.83-1.77 (quin, J = 6.8 Hz, 4H, 2 × Ar-O-CH_2-C$\underline{H}_2$-), 1.49-1.23 (m, 28H, 2 × -$(CH_2)_7$-), 0.88 (t, J = 7 Hz, 6H, 2 × -CH_3); Elemental analysis: $C_{66}H_{76}O_{10}$ requires C 77.01, H 7.43; found C 76.64, H 7.21%.

2,7-Naphthylene bis(4-(E-4-*n*-dodecyloxy-α-methylcinnamoyloxy)-3-methylbenzoate), 6.B.7

Yield: (62%); mp 114 °C; IR (KBr) ν_{max}: 3056, 2950, 2920, 2850, 1733, 1725, 1631, 1608, 1508, 1456, 1377 cm^{-1}; ^{1}H NMR (400 MHz, $CDCl_3$) δ: 8.19-8.14 (m, 4H, Ar-H), 7.97-7.94 (m, 4H, Ar-H), 7.69 (d, J = 1.63 Hz, 2H, Ar-H), 7.49 (d, J = 8.66 Hz, 4H, Ar-H), 7.37 (dd, J_1 = 2 Hz, J_2 = 6.79 Hz, 2H, Ar-H), 7.29-7.27 (m, 2H, Ar-H), 6.98 (d, J = 8.71 Hz, 4H, Ar-H), 4.01 (t, J = 6.52 Hz, 4H, 2 × Ar-O-CH_2-), 2.34 (s, 6H, 2 × -Ar-CH_3), 2.3 (d, 6H, 2 × -CH=C(C$\underline{H}_3$)COO-), 1.83-1.77 (quin, J = 7.68 Hz, 4H, 2 × Ar-O-CH_2-C$\underline{H}_2$-), 1.51-1.23 (m, 36H, 2 × -$(CH_2)_9$-), 0.88 (t, J = 6.43 Hz, 6H, 2 × -CH_3); Elemental analysis: $C_{70}H_{84}O_{10}$ requires C 77.46, H 7.79; found C 77.75, H 8.2%.

2,7-Naphthylene bis(4-(E-4-*n*-tridecyloxy-α-methylcinnamoyloxy)-3-methylbenzoate), 6.B.8

Yield: (59%); mp 111.5 °C; IR (KBr) ν_{max}: 3058, 2958, 2922, 2852, 1730, 1727, 1627, 1608, 1504, 1454, 1377 cm^{-1}; ^{1}H NMR (400 MHz, $CDCl_3$) δ: 8.19-8.14 (m, 4H, Ar-H), 7.96-7.94 (m, 4H, Ar-H), 7.69 (d, J = 2.12 Hz, 2H, Ar-H), 7.48 (d, J = 8.74 Hz, 4H, Ar-H), 7.38 (dd, J_1 = 2.1 Hz, J_2 = 6.71 Hz, 2H, Ar-H), 7.29-7.27 (m, 2H, Ar-H), 6.97 (d, J = 8.76 Hz, 4H, Ar-H), 4.01 (t, J = 6.8 Hz, 4H, 2 × Ar-O-CH_2-), 2.34 (s, 6H, 2 × -Ar-CH_3), 2.3 (d, 6H, 2 × -CH=C(C$\underline{H}_3$)COO-), 1.84-1.77 (quin, J = 6.76 Hz, 4H, 2 × Ar-O-CH_2-C$\underline{H}_2$-), 1.51-1.24 (m, 40H, 2 × -$(CH_2)_{10}$-), 0.88 (t, J = 6.46 Hz, 6H, 2 × -CH_3); Elemental analysis: $C_{72}H_{88}O_{10}$ requires C 77.66, H 7.97; found C 77.83, H 8.28%.

2,7-Naphthylene bis(4-(E-4-*n*-tetradecyloxy-α-methylcinnamoyloxy)-3-methylbenzoate), 6.B.9

Yield: (57%); mp 111.5 °C; IR (KBr) ν_{max}: 3056, 2921, 2850, 1732, 1725, 1628, 1604, 1504, 1454, 1377 cm^{-1}; ^{1}H NMR (400 MHz, $CDCl_3$) δ: 8.19-8.13 (m, 4H, Ar-H), 7.95-7.93 (m, 4H, Ar-H), 7.69 (d, J = 1.8 Hz, 2H, Ar-H), 7.48 (d, J = 8.72 Hz, 4H, Ar-H), 7.38 (dd, J_1 = 1.9

Hz, J_2 = 6.74 Hz, 2H, Ar-H), 7.29-7.27 (m, 2H, Ar-H), 6.98 (d, J = 6.23 Hz, 4H, Ar-H), 4.01 (t, J = 6.5 Hz, 4H, 2 × Ar-O-CH_2-), 2.34 (s, 6H, 2 × -Ar-CH_3), 2.3 (d, 6H, 2 × -CH=C(C$\underline{H}_3$)COO-), 1.84-1.77 (quin, J = 6.6 Hz, 4H, 2 × Ar-O-CH_2-C$\underline{H}_2$-), 1.55-1.26 (m, 44H, 2 × -$(CH_2)_{11}$-), 0.88 (t, J = 6.5 Hz, 6H, 2 × -CH_3); Elemental analysis: $C_{74}H_{92}O_{10}$ requires C 77.86, H 8.11; found C 77.91, H 8.48%.

2,7-Naphthylene bis(4-(E-4-*n*-hexadecyloxy-α-methylcinnamoyloxy)-3-methylbenzoate), 6.B.10

Yield: (60%); mp 116.5 °C; IR (KBr) ν_{max}: 3056, 2950, 2921, 2852, 1730, 1727, 1627, 1608, 1504, 1456, 1377 cm^{-1}; ^{1}H NMR (400 MHz, $CDCl_3$) δ: 8.19-8.14 (m, 4H, Ar-H), 7.96-7.94 (m, 4H, Ar-H), 7.69 (d, J = 2.12 Hz, 2H, Ar-H), 7.48 (d, J = 8.98 Hz, 4H, Ar-H), 7.38 (dd, J_1 = 2 Hz, J_2 = 6.88 Hz, 2H, Ar-H), 7.29-7.27 (m, 2H, Ar-H), 6.98 (d, J = 8.7 Hz, 4H, Ar-H), 4.01 (t, J = 6.54 Hz, 4H, 2 × Ar-O-CH_2-), 2.34 (s, 6H, 2 × -Ar-CH_3), 2.3 (d, 6H, 2 × -CH=C(C$\underline{H}_3$)COO-), 1.82-1.77 (quin, J = 6.8 Hz, 4H, 2 × Ar-O-CH_2-C$\underline{H}_2$-), 1.51-1.24 (m, 52H, 2 × -$(CH_2)_{13}$-), 0.88 (t, J = 6.6 Hz, 6H, 2 × -CH_3); Elemental analysis: $C_{78}H_{100}O_{10}$ requires C 78.23, H 8.4; found C 78, H 8.51%.

References

[1] Pelzl, G.; Diele, S.; Weissflog, W. *Adv. Mater.* **1999**, *11*, 707-724.

[2] Reddy, R. A.; Tschierske, C. *J. Mater. Chem.* **2006**, *16*, 907-961.

[3] Takezoe, H.; Takanishi, Y. *Jpn. J. Appl. Phys.* **2006**, *45*, 597-625.

[4] Niori, T.; Sekine, T.; Watanabe, J.; Furukawa, T.; Takezoe, H. *J. Mater. Chem.* **1996**, *6*, 1231-1233.

[5] Link, D. R.; Natale, G.; Shao, R.; Maclennan, J. E.; Clark, N. A.; Korblova, E.; Walba, D. M. *Science* **1997**, *278*, 1924-1927.

[6] Weissflog, W.; Nadasi, H.; Dunemann, U.; Pelzl, G.; Diele, S.; Eremin, A.; Kresse, H. *J. Mater. Chem.* **2001,** *11*, 2748-2758.

[7] Wirth, I.; Diele, S.; Eremin, A.; Pelzl, G.; Grande, S.; Kovalenko, N.; Pancenko, N.; Weissflog, W. *J. Mater. Chem.* **2001,** *11*, 1642-1650.

[8] Dunemann, U.; Schroder, M. W.; Reddy, R. A.; Pelzl, G.; Diele, S.; Weissflog, W. *J. Mater. Chem.* **2005,** *15*, 4051-4061.

[9] Sadashiva, B. K.; Raghunathan, V. A.; Pratibha, R. *Ferroelectrics* **2000,** *243*, 249-260.

[10] Murthy, H. N. S.; Sadashiva, B. K. *Liq. Cryst.* **2002,** *29*, 1223-1234.

[11] Reddy, R. A.; Sadashiva, B. K. *Liq. Cryst.* **2003,** *30*, 1031-1050.

[12] Pelzl, G.; Eremin, A.; Diele, S.; Kresse, H.; Weissflog, W. *J. Mater. Chem.* **2002**, *12*, 2591-2593.

[13] Gortz, V.; Southern, C.; Roberts, N. W.; Gleeson, H. F.; Goodby, J. W. *Soft Matter* **2009**, *5*, 463-471.

[14] Reddy, R. A.; Sadashiva, B. K.; Surajit, D. *Chem. Commun.* **2001,** 1972-1973.

[15] Reddy, R. A.; Sadashiva, B. K.; Raghunathan, V. A. *Chem. Mater.* **2004,** *16*, 4050-4062.

[16] Reddy, R. A.; Sadashiva, B. K. *Liq. Cryst.* **2000,** *27*, 1613-1623.

[17] Reddy, R. A.; Sadashiva, B. K. *J. Mater. Chem.* **2004**, *14*, 1936-1947.

[18] Reddy, R. A.; Raghunathan, V. A.; Sadashiva, B. K. *Chem. Mater.* **2005,** *17*, 274-283.

[19] Murthy, H. N. S.; Sadashiva, B. K. *Liq. Cryst.* **2004,** *31*, 1347-1356.

[20] Svoboda, V; Novotna, V.; Kozmik, J.; Pociecha, D.; Glogarova, M.; Weissflog, W.; Diele, S.; Pelzl, G. *J. Mater. Chem.* **2003,** *13*, 2104-2110.

[21] Kohout, M.; Scoboda, J.; Novotan, V.; Poiecha, D.; Glogarova, M.; Gorecka, E. *J. Mater. Chem.* **2009**, *19*, 3153-3160.

[22] Sadashiva, B. K. *Mol. Cryst. Liq. Cryst.* **1979**, *53*, 253-262.

[23] Johnson, J. R. In *Organic Reactions*, Vol.1, Eds. Adams, R., Bachmann, W. E., Fieser, L. F., Snyder, J. R. John Wiley & Sons, New York, p.210 (1942).

[24] Tamba, M. G.; Baumeister, U.; Pelzl, G.; Weissflog, W. *Liq. Cryst.* **2010,** *37*, 853-874.

[25] Wiant, D.; Gleeson, J. T.; Éber, N.; Fodor-Csorba, K.; Jákli, A.; Tóth-Katona, T. *Phys. Rev. E* **2005,** *72*, 041712.